Electronic Supplementary Material (ESI) for Journal of Materials Chemistry B.

Supplementary Information

For

Magnetic nanomaterials with near-infrared pH-activatable fluorescence *via* iron-catalyzed AGET ATRP for tumor acidic microenvironment imaging†

Xiaodong Liu,[a] Qian Chen[b], Guangbao Yang[b], Lifen Zhang,[a] Zhuang Liu,[*b]
Zhenping Cheng[*a] and Xiulin Zhu[a]

[a] *Suzhou key Laboratory of Macromolecular Design and Precision Synthesis, Jiangsu Key Laboratory of Advanced Functional Polymer Design and Application, Department of Polymer Science and Engineering, College of Chemistry, Chemical Engineering and Materials Science, Soochow University, Suzhou 215123, China.*

[b] *Institute of Functional Nano and Soft Materials (FUNSOM) and Jiangsu Key Laboratory for Carbon-Based Functional Materials and Devices, Soochow University, Suzhou 215123, China.*

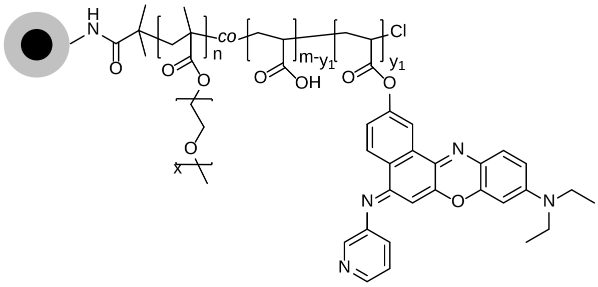

$Fe_3O_4@SiO_2@PPEGMA_{475}$-*co*-PAA@Oxazine-1

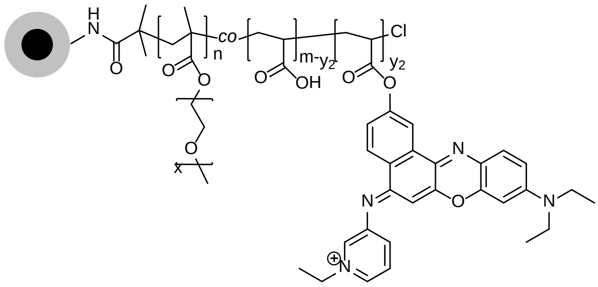

$Fe_3O_4@SiO_2@PPEGMA_{475}$-*co*-PAA@Oxazine-2

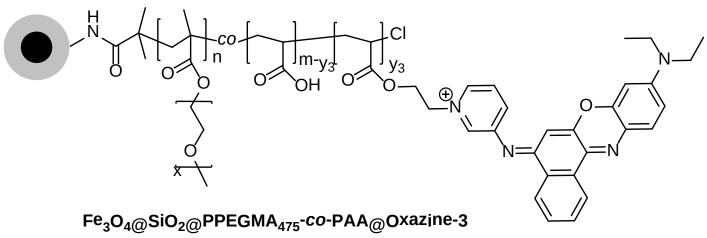

$Fe_3O_4@SiO_2@PPEGMA_{475}$-*co*-PAA@Oxazine-3

Fig. S1 Structures of benzo[*a*]phenoxazine-dotted $Fe_3O_4@SiO_2@PPEGMA_{475}$-*co*-PAA@Oxazine MNPs.

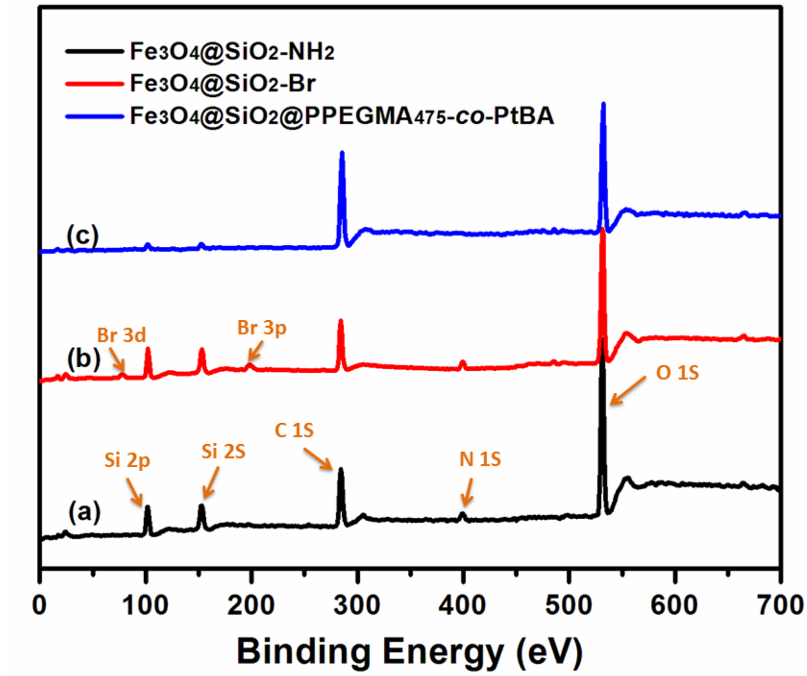

Fig. S2 XPS spectra of MNPs of (a) $Fe_3O_4@SiO_2$-NH_2, (b) $Fe_3O_4@SiO_2$-Br and (c) $Fe_3O_4@SiO_2@PPEGMA_{475}$-*co*-PtBA.

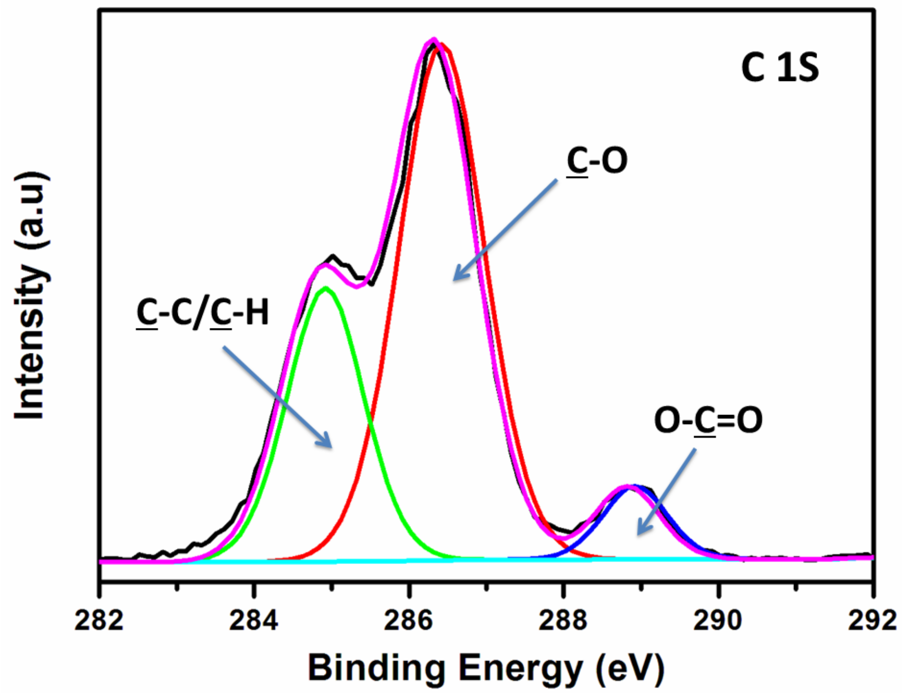

Fig. S3 XPS C 1s core-level spectra of Fe_3O_4@SiO_2@PPEGMA$_{475}$-*co*-PtBA.

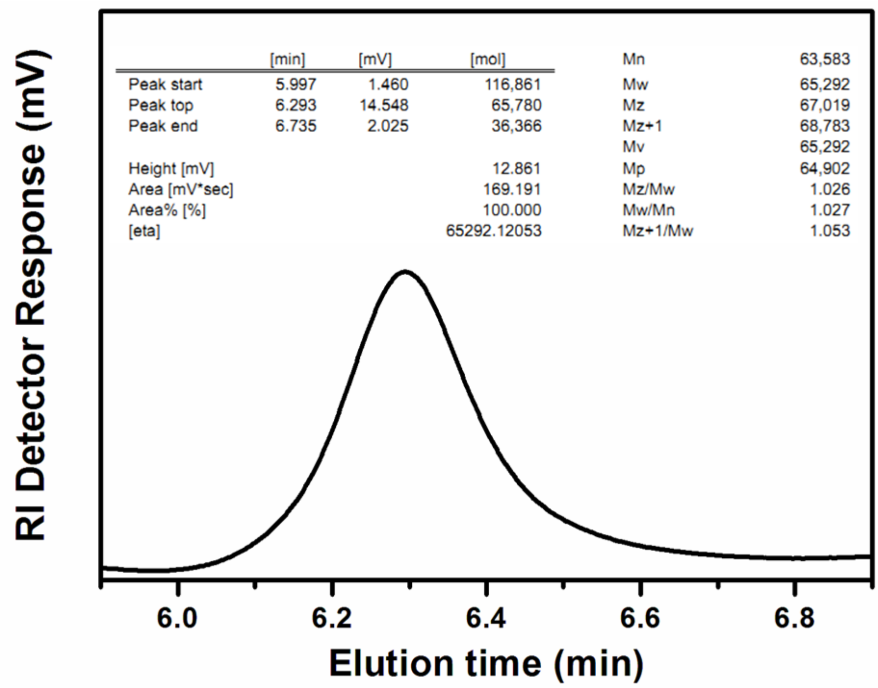

Fig. S4 GPC curve and data of PPEGMA$_{475}$-*co*-PtBA grafted on the surface of Fe_3O_4@SiO_2@PPEGMA$_{475}$-*co*-PtBA. The sample was obtained by etching with hydrofluoric acid from corresponding MNPs.

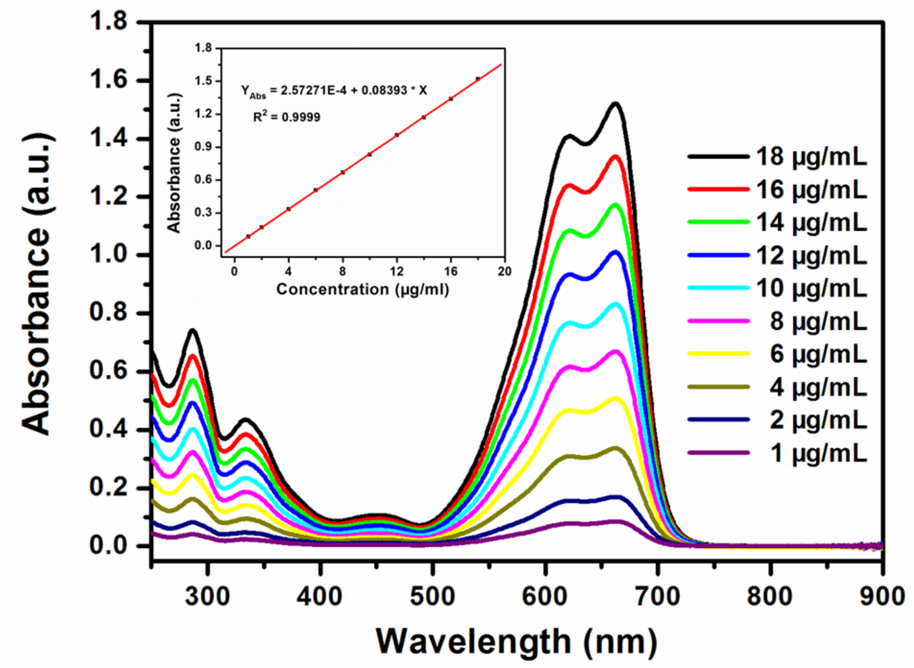

Fig. S5 Absorption spectra of **3a** (1, 2, 4, 6, 8, 10, 12, 14, 16 and 18 μg/mL) in Na_2HPO_4-citric acid buffer solution (pH 3.0); inset shows the linear fit of absorbance at 665 nm.

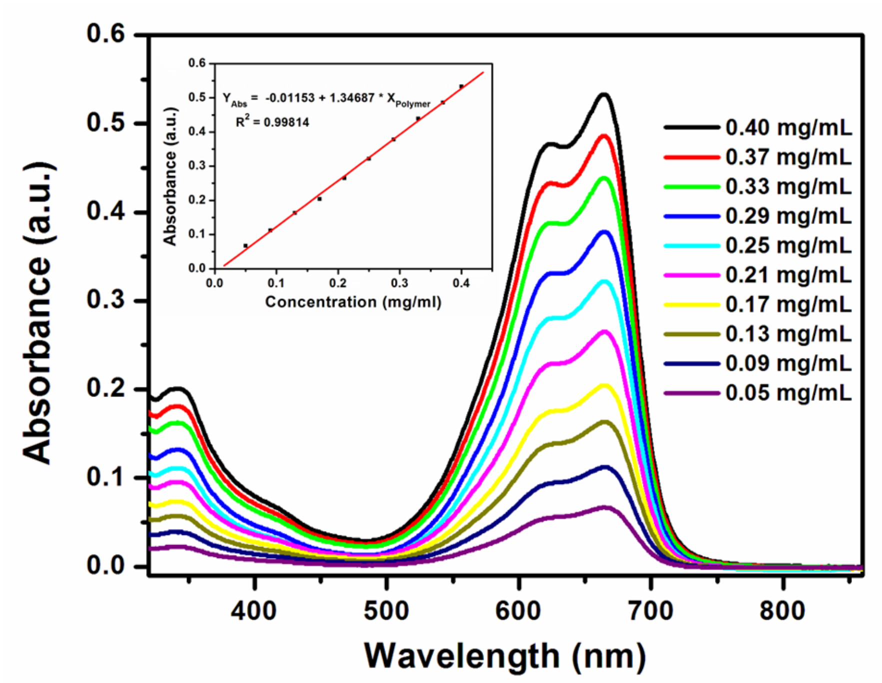

Fig. S6 Absorption spectra of PPEGMA$_{475}$-*co*-PAA@Oxazine-2 (0.05, 0.09, 0.13, 0.17, 0.21, 0.25, 0.29, 0.33, 0.37 and 0.40 mg/mL) in Na_2HPO_4-citric acid buffer solution (pH 3.0); inset shows the linear fit of absorbance at 665 nm.

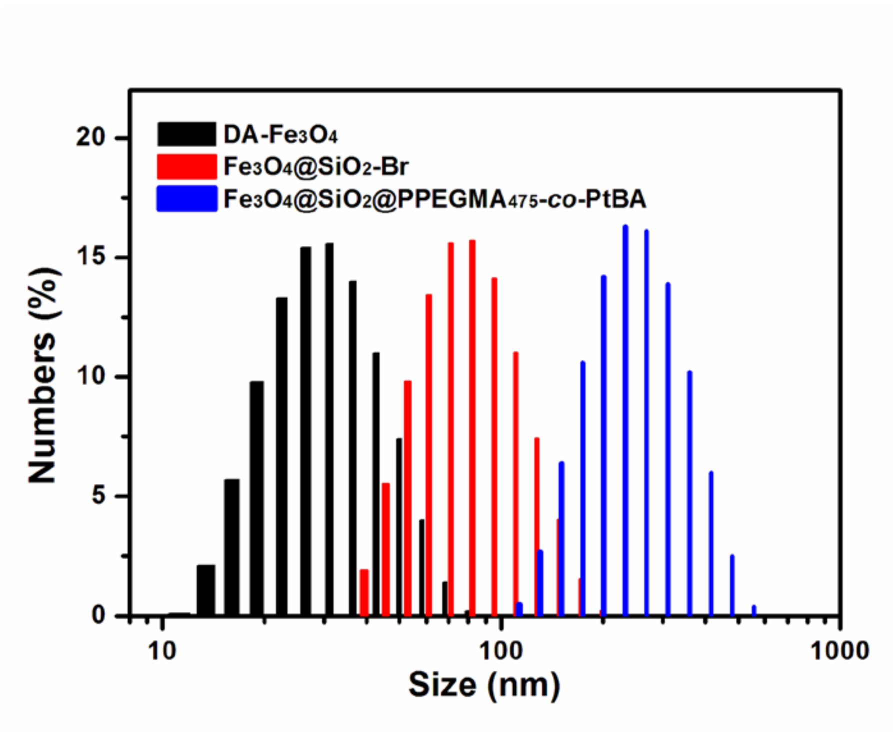

Fig. S7 Particle sizes of the as-prepared MNPs at different modification stages in water by DLS.

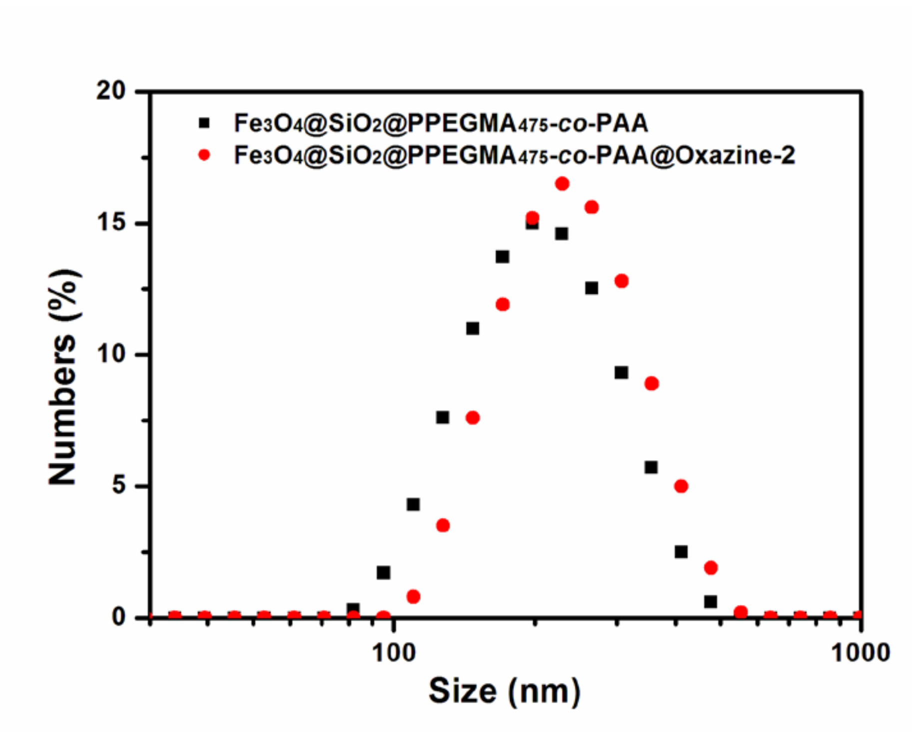

Fig. S8 Particle sizes of the as-prepared MNPs at different modification stages in water by DLS.

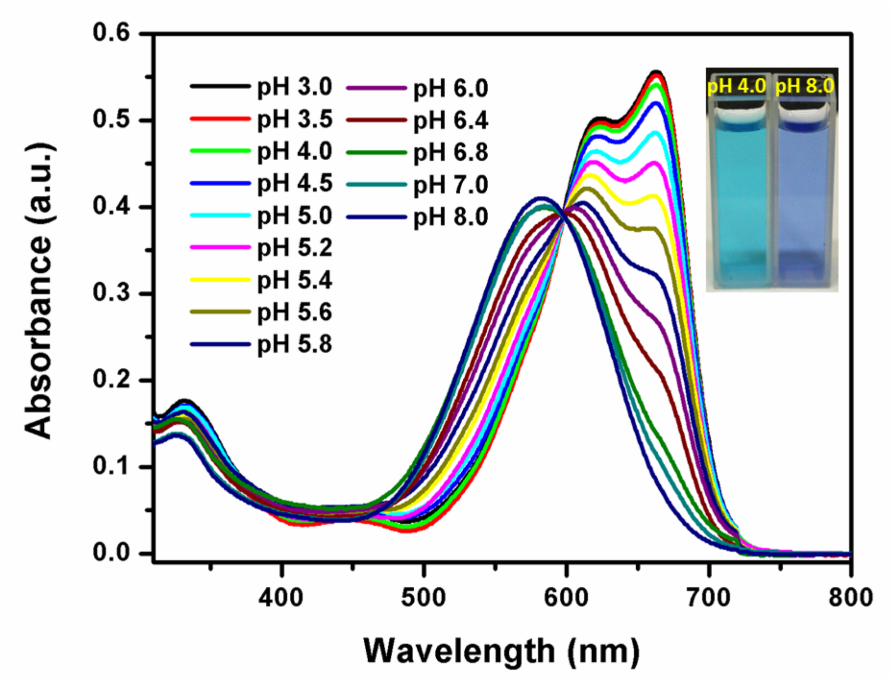

Fig. S9 Absorption properties of compound **3a** (10 μM) toward different pH values in Na_2HPO_4-citric acid buffer solution with 10% DMSO as a co-solvent.

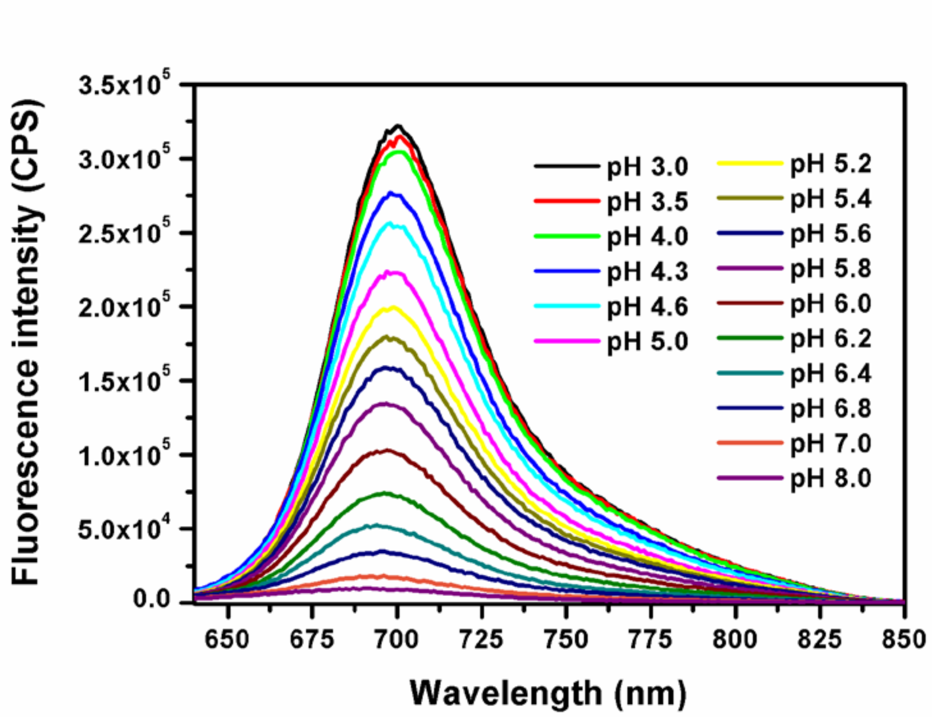

Fig. S10 Absorption properties of compound **3a** (10 μM) toward different pH values in Na_2HPO_4-citric acid buffer solution with 10% DMSO as a co-solvent (λex = 600 nm).

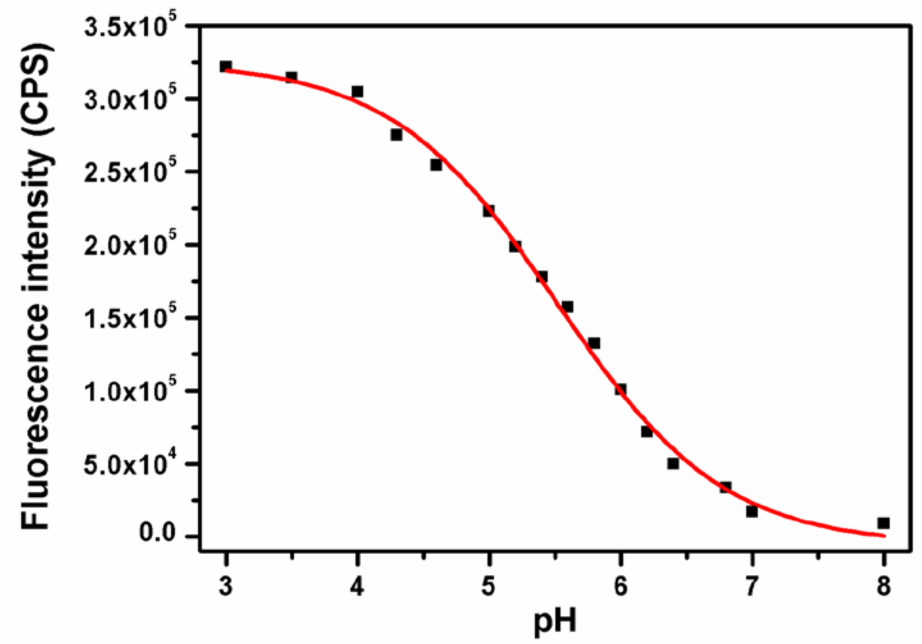

Fig. S11 Fluorescence intensity changes of compound **3a** (10 μM) at 700 nm toward different pH values in Na_2HPO_4-citric acid buffer solution with 10% DMSO as a co-solvent.

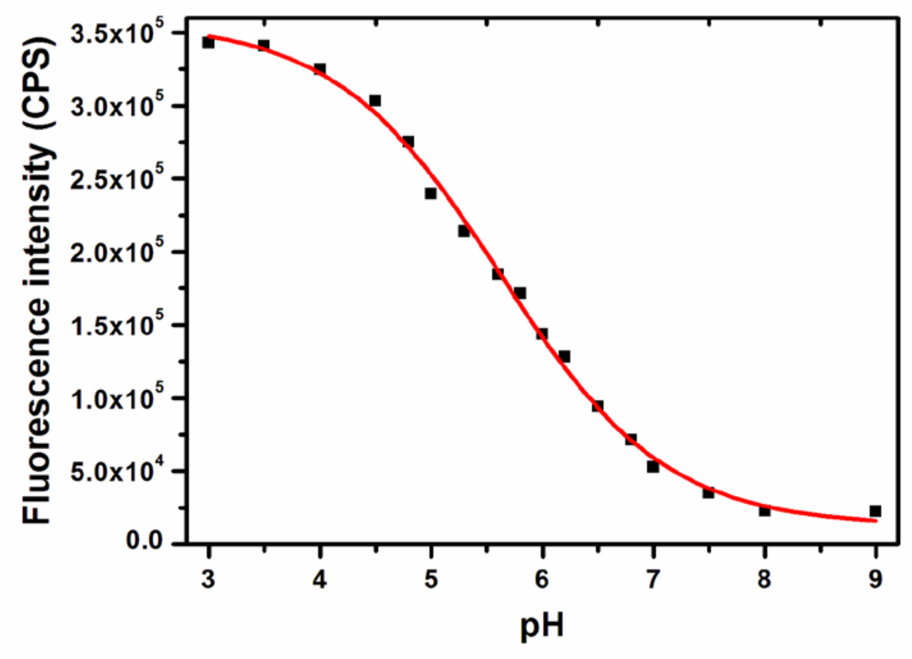

Fig. S12 Fluorescence intensity changes at 688 nm of Fe_3O_4@SiO_2@$PPEGMA_{475}$-*co*-PAA@Oxazine-2 toward different pH values in Na_2HPO_4-citric acid buffer solution.

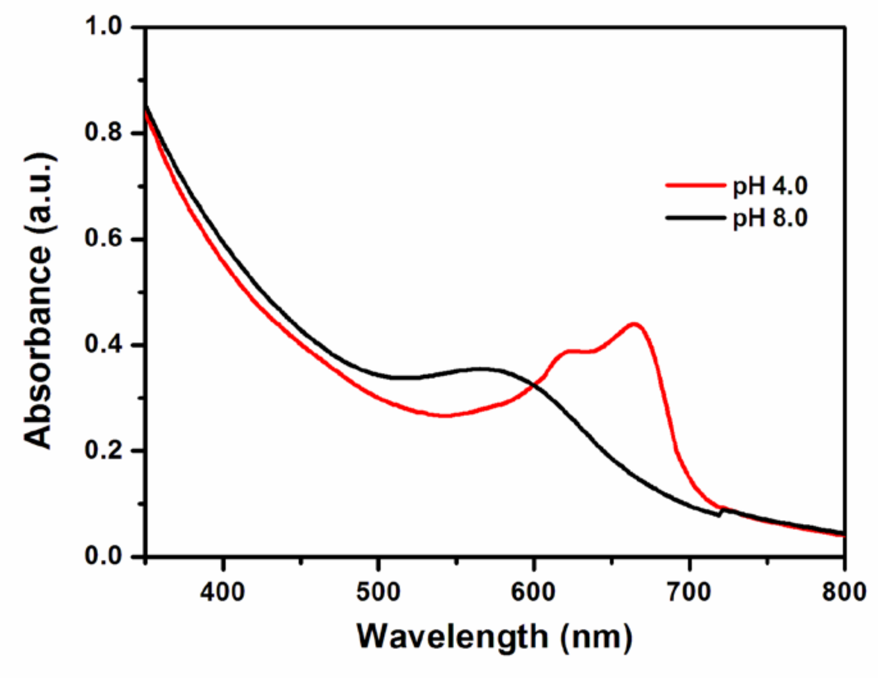

Fig. S13 Absorption properties of Fe_3O_4@SiO_2@PPEGMA$_{475}$-*co*-PAA@Oxazine-2 toward different pH values in Na_2HPO_4-citric acid buffer solution. (Iron concentrations is 0.025 mg/mL, λex = 600 nm).

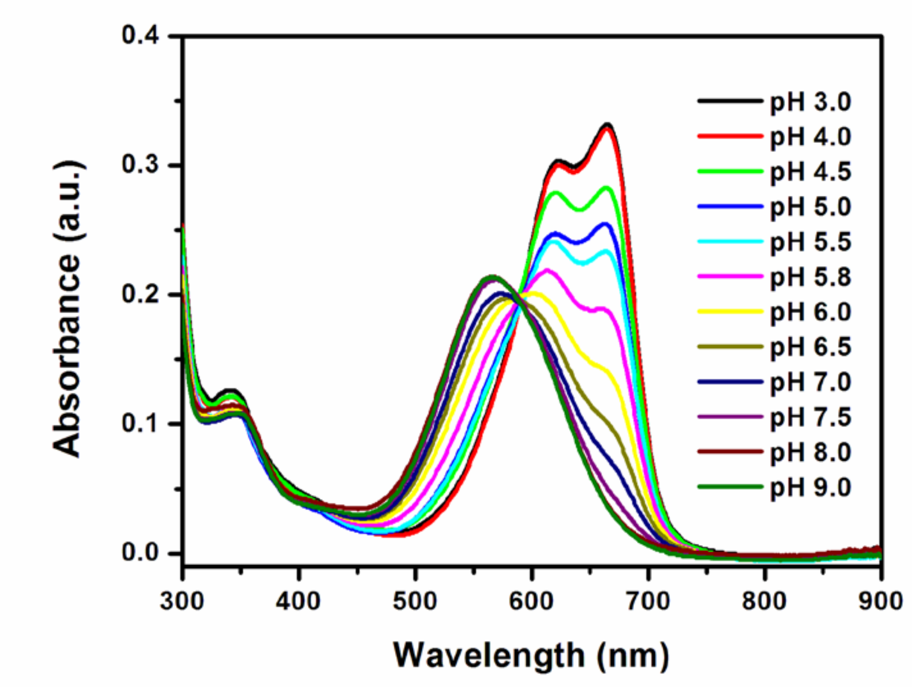

Fig. S14 Absorption spectra of grafted polymer PPEGMA$_{475}$-*co*-PAA@Oxazine-2 (0.25 mg/mL) toward different pH values in Na_2HPO_4-citric acid buffer solution. The polymer was collected from the hybrid Fe_3O_4@SiO_2@PPEGMA$_{475}$-*co*-PAA@Oxazine-2 MNPs after treated with HF to remove the Fe_3O_4@SiO_2 core.

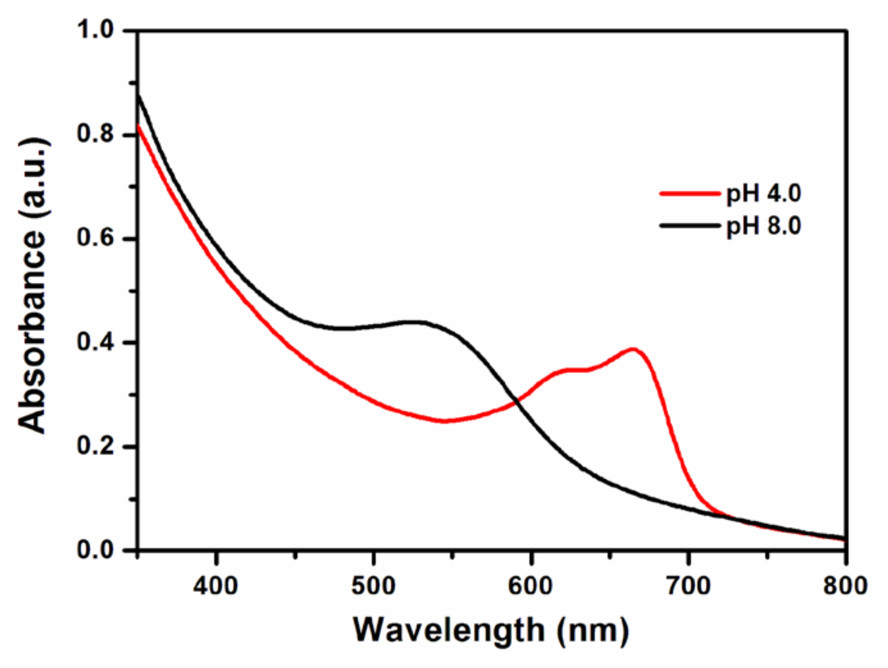

Fig. S15 Absorption properties of Fe_3O_4@SiO_2@PPEGMA$_{475}$-*co*-PAA@Oxazine-1 toward different pH values in Na_2HPO_4-citric acid buffer solution. (Iron concentrations is 0.025 mg/mL, λex = 600 nm).

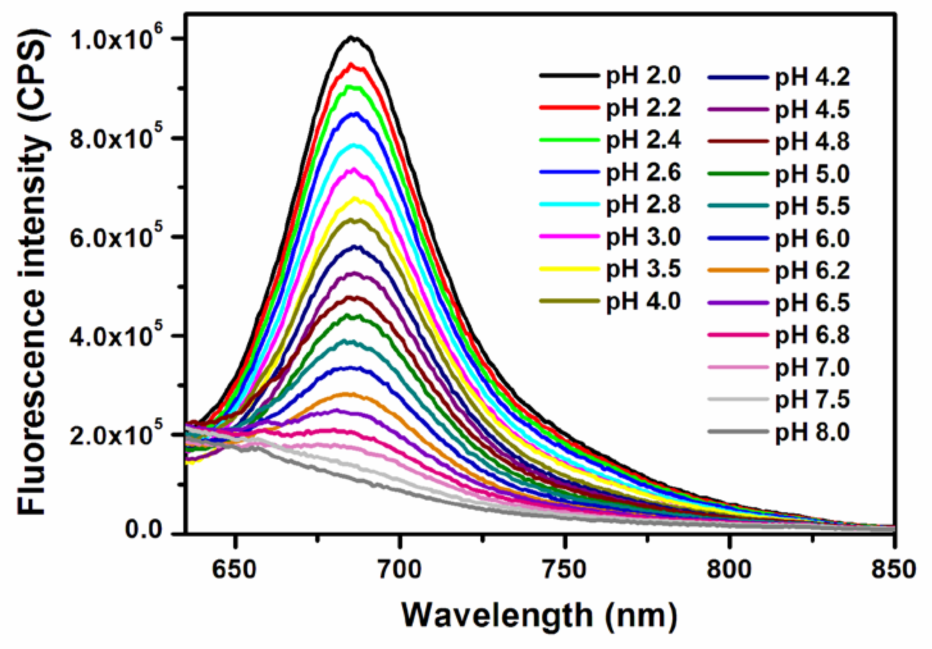

Fig. S16 Emission properties of Fe_3O_4@SiO_2@PPEGMA$_{475}$-*co*-PAA@Oxazine-1 toward different pH values in Na_2HPO_4-citric acid buffer solution. (Iron concentrations is 0.025 mg/mL, λex = 600 nm).

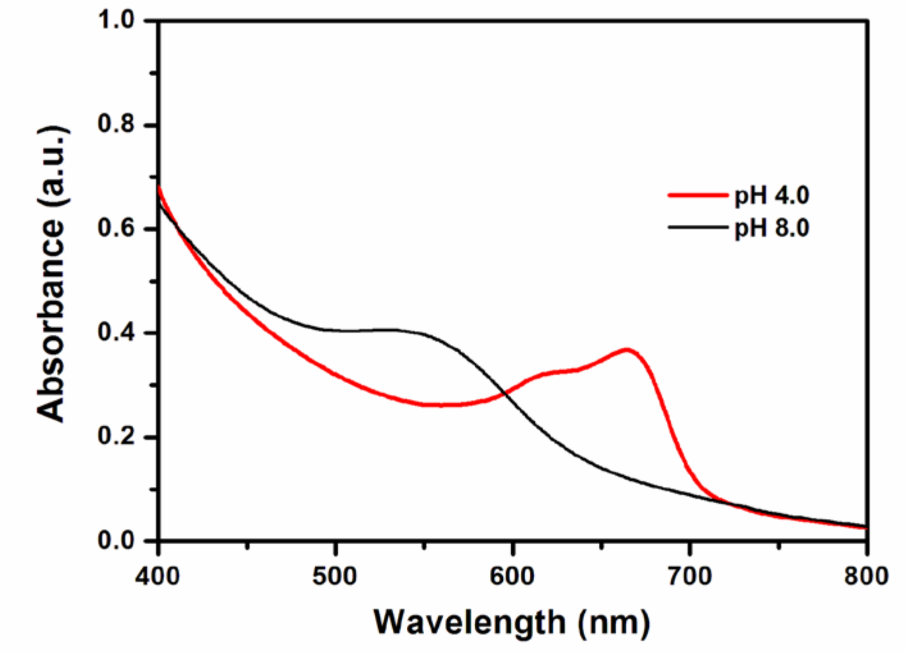

Fig. S17 Absorption properties of Fe_3O_4@SiO_2@PPEGMA$_{475}$-*co*-PAA@Oxazine-3 toward different pH values in Na_2HPO_4-citric acid buffer solution. (Iron concentrations is 0.025 mg/mL, λex = 600 nm).

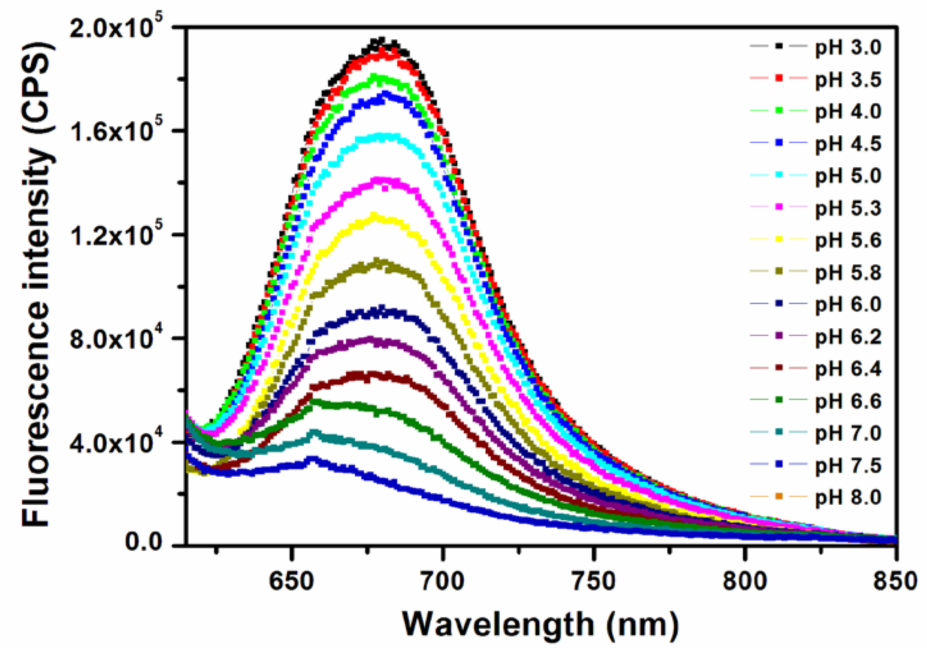

Fig. S18 Emission properties of Fe_3O_4@SiO_2@PPEGMA$_{475}$-*co*-PAA@Oxazine-3 toward different pH values in Na_2HPO_4-citric acid buffer solution. (Iron concentrations is 0.012 mg/mL, λex = 600 nm).

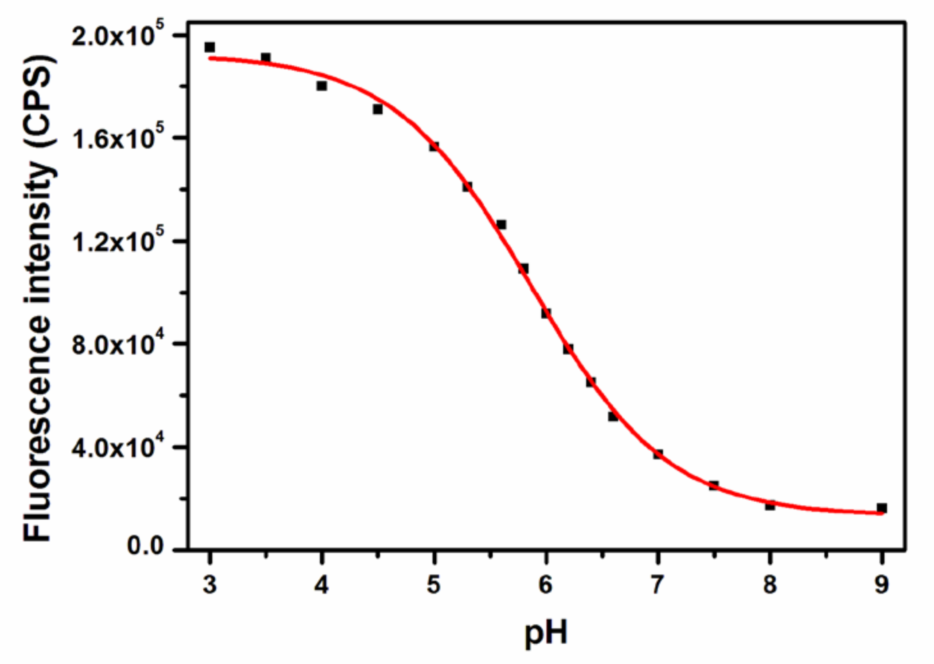

Fig. S19 Fluorescence intensity changes at 680 nm of Fe_3O_4@SiO_2@PPEGMA$_{475}$-*co*-PAA@Oxazine-3 toward different pH values in Na_2HPO_4-citric acid buffer solution.

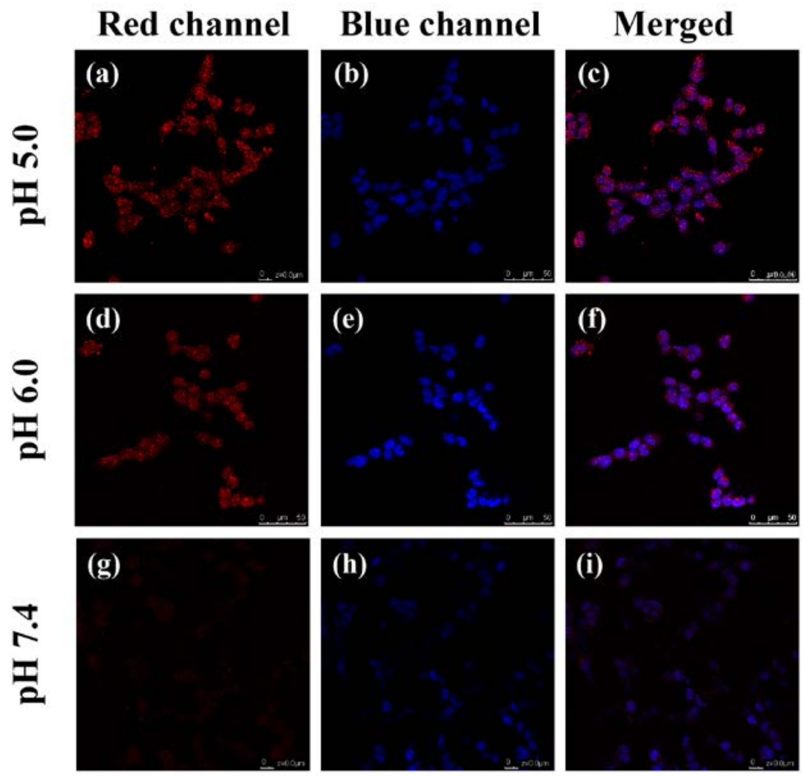

Fig. S20 Confocal fluorescent images of fixed 293T cells incubated with Fe_3O_4@SiO_2@PPEGMA$_{475}$-*co*-PAA@Oxazine-2 and Hoechst 33342 at pH 5.0 (a-c), pH 6.0 (d-f), and pH 7.4 (g-i), respectively.

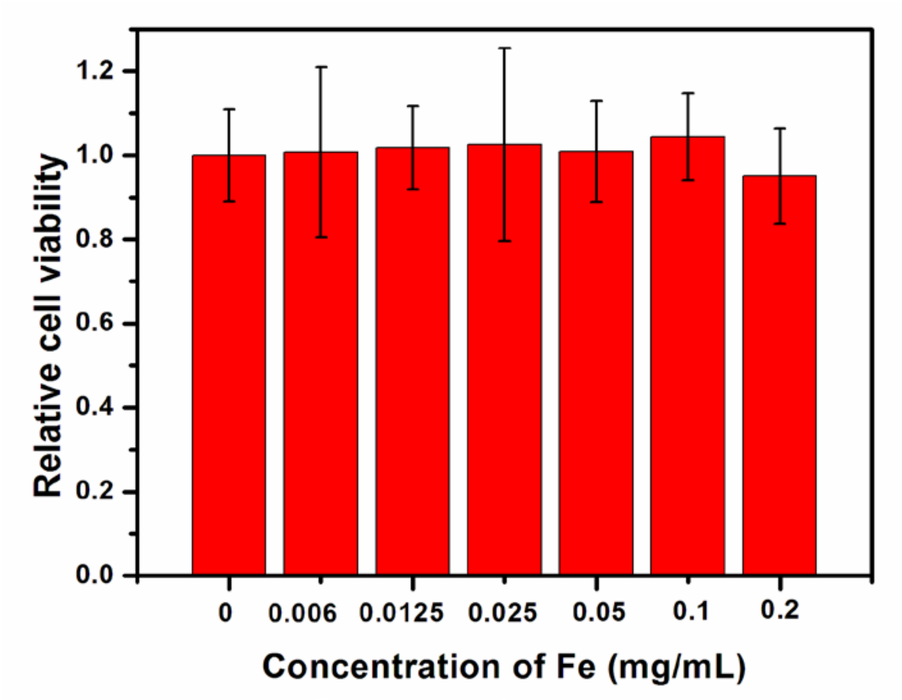

Fig. S21 Relative cell viability data of 4T1 cells incubated with a series of iron concentrations of Fe_3O_4@SiO_2@$PPEGMA_{475}$-*co*-PAA@Oxazine-2 measured by the MTT cell viability assay.

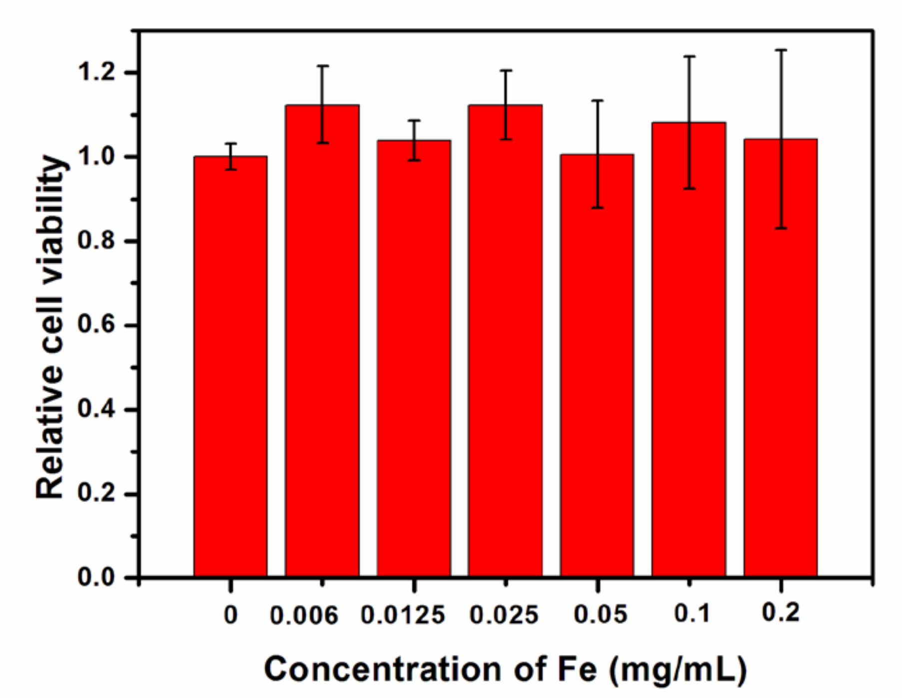

Fig. S22 Relative cell viability data of 293T cells incubated with a series of iron concentrations of Fe_3O_4@SiO_2@$PPEGMA_{475}$-*co*-PAA@Oxazine-2 measured by the MTT cell viability assay.

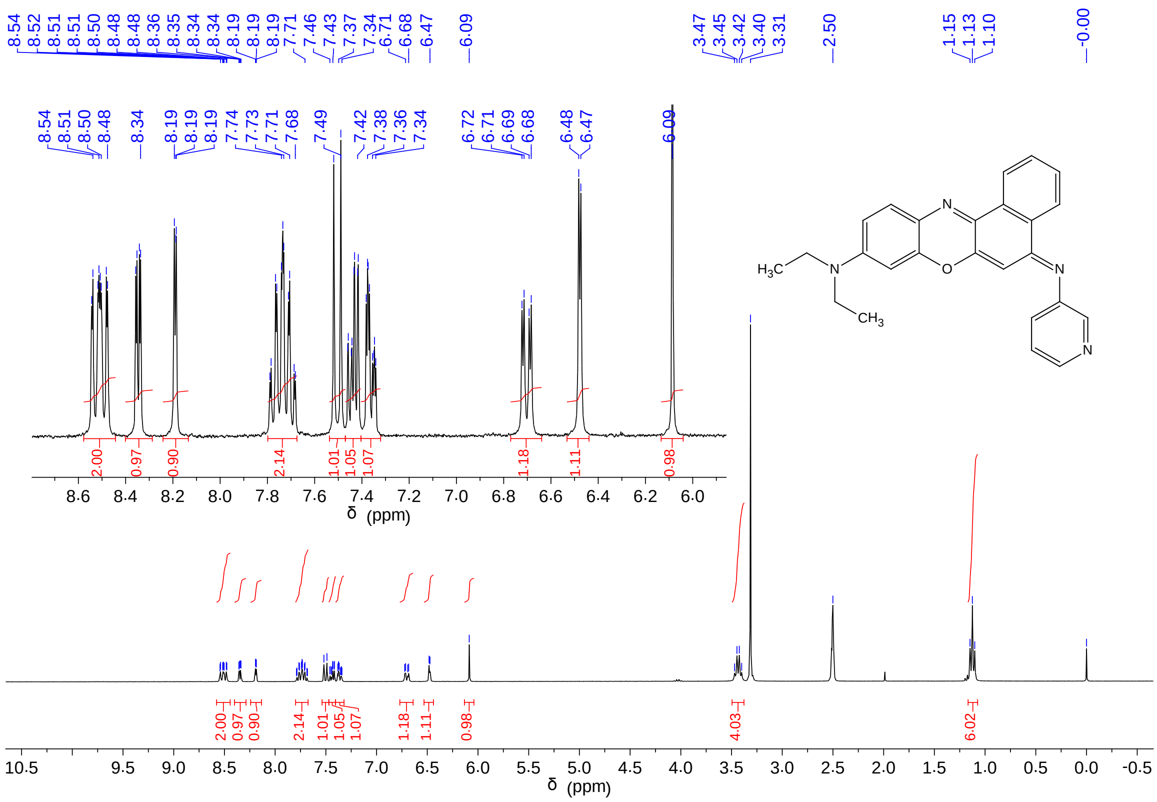

Fig. S23 [1]H NMR (300 MHz) of **2a** in DMSO-d_6.

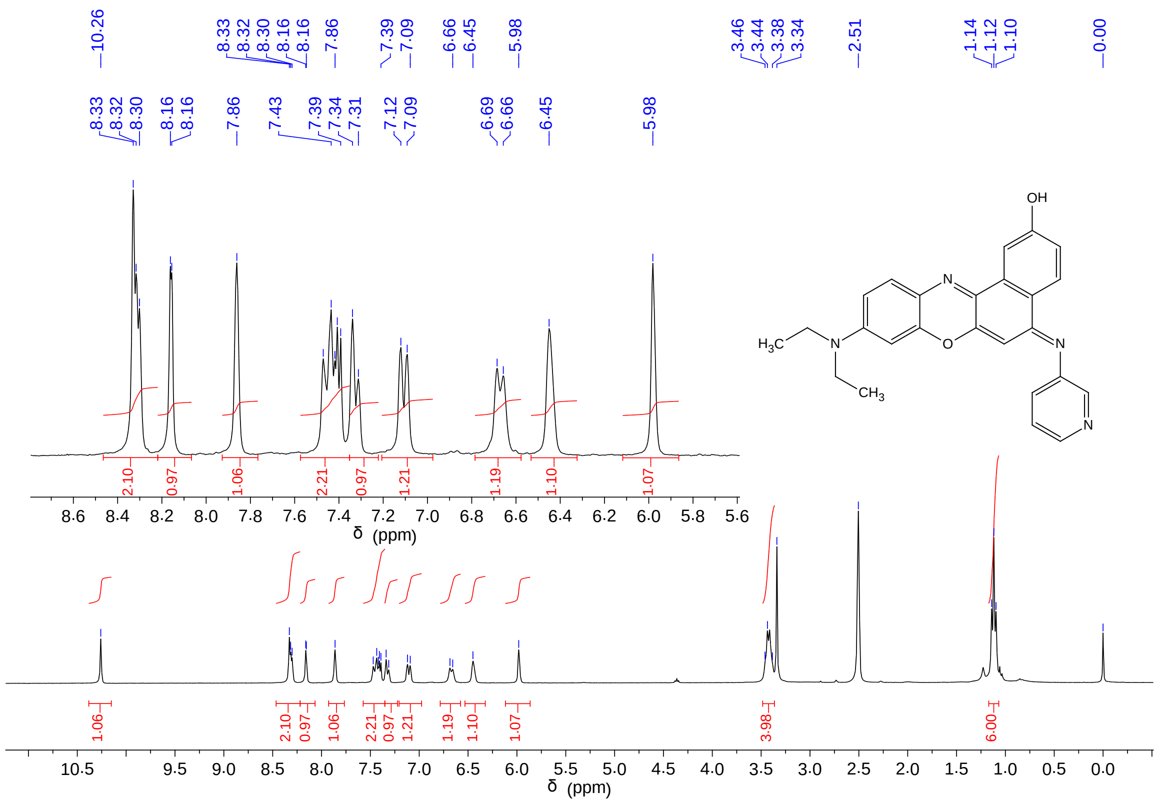

Fig. S24 [1]H NMR (300 MHz) of **2b** in DMSO-d_6.

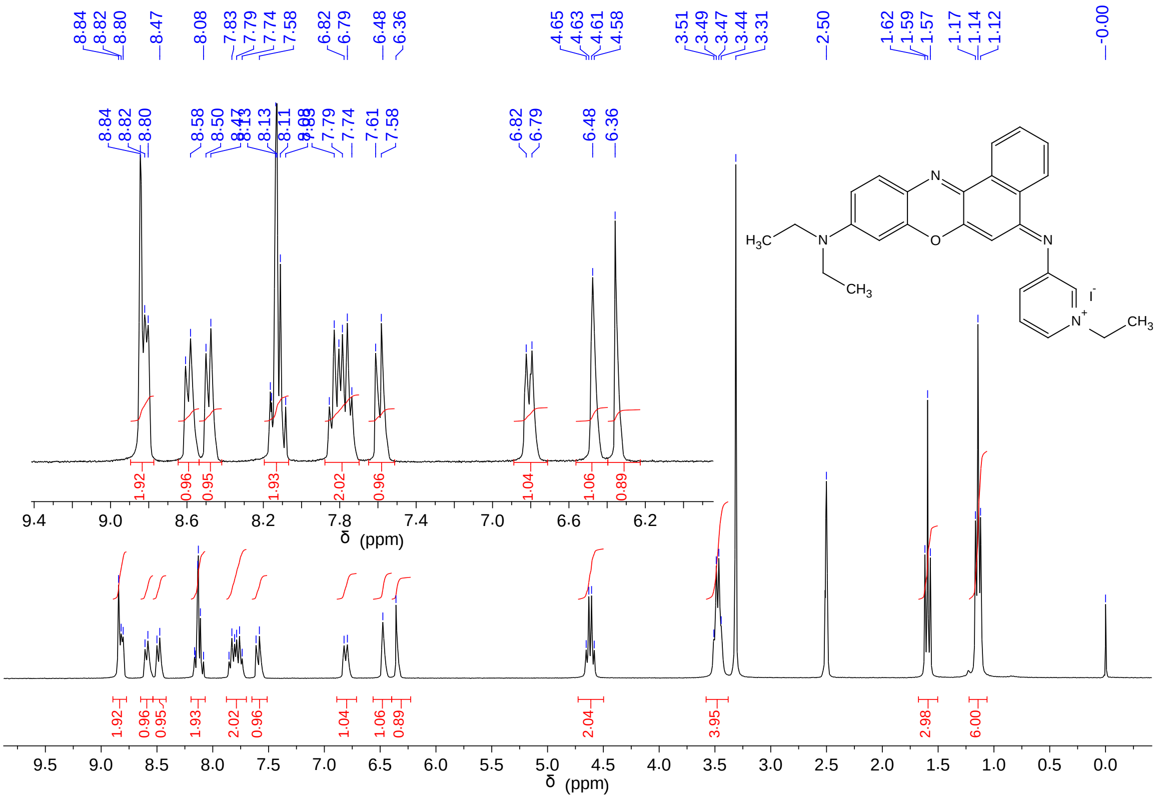

Fig. S25 [1]H NMR spectra (300 MHz) of **3a** in DMSO-d_6.

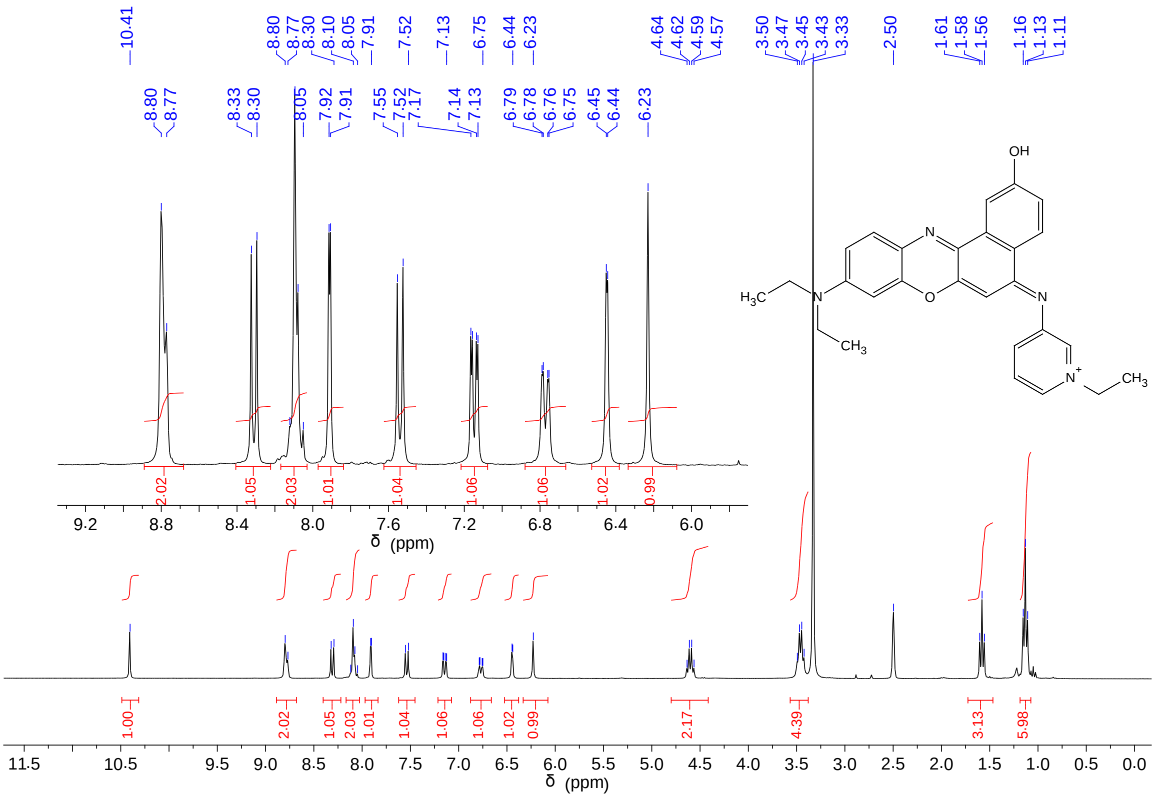

Fig. S26 [1]H NMR spectra (300 MHz) of **3b** in DMSO-d_6.

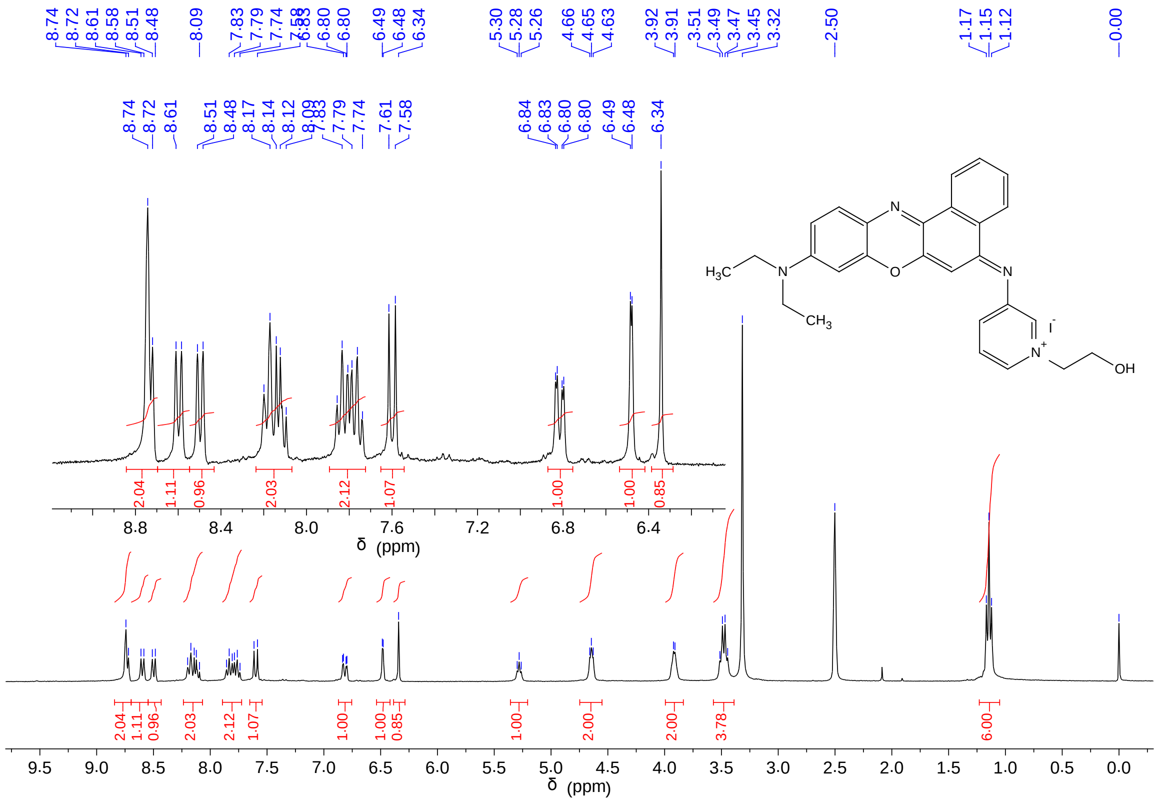

Fig. S27 ^{1}H NMR (300 MHz) of **3c** in DMSO-d_6.

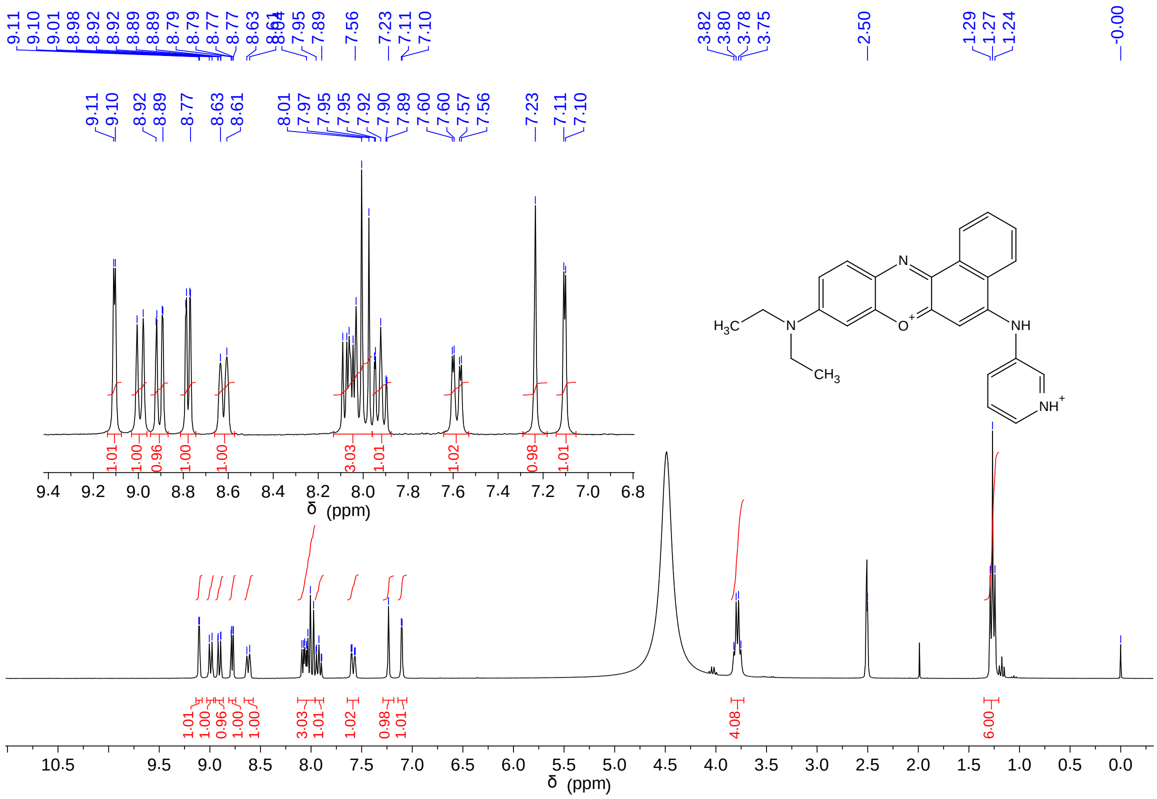

Fig. S28 ^{1}H NMR spectra (300 MHz) of **2a+H$^+$** in DMSO-d_6.

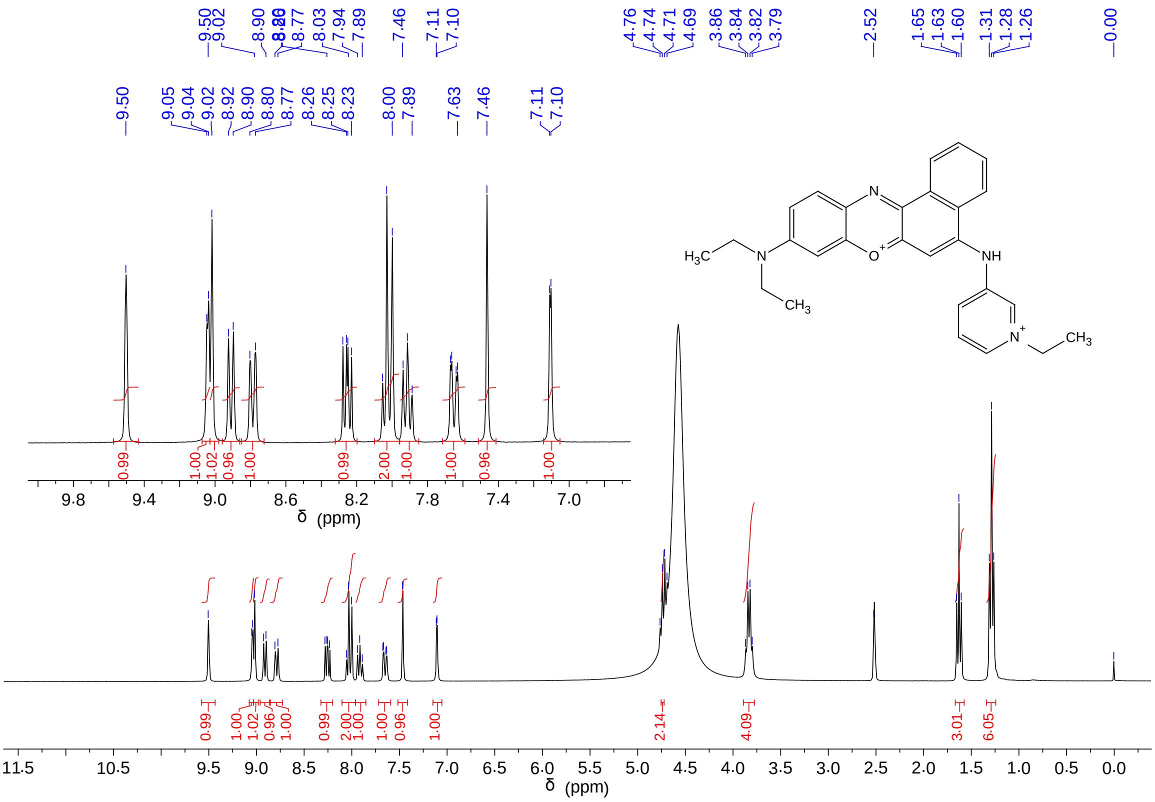

Fig. S29 ^{1}H NMR spectra (300 MHz) of **3a+H^{+}** in DMSO-d_6.

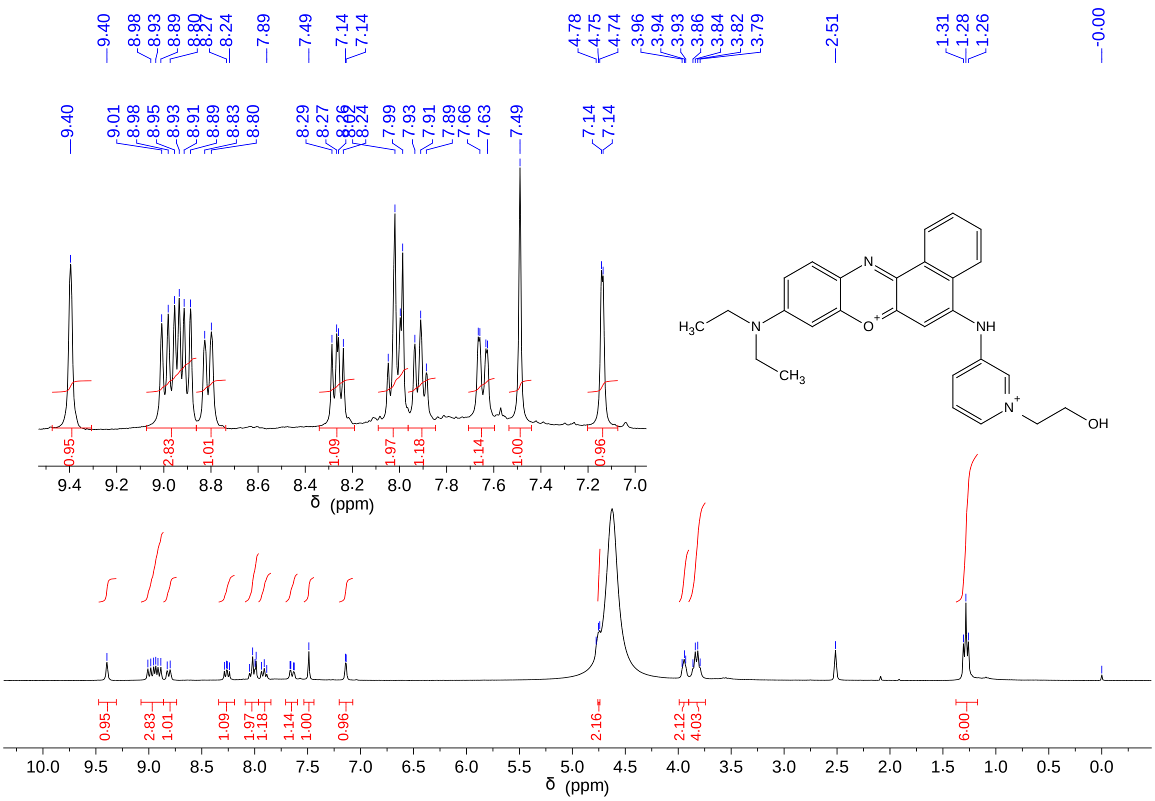

Fig. S30 ^{1}H NMR spectra (300 MHz) of **3c+H^{+}** in DMSO-d_6.

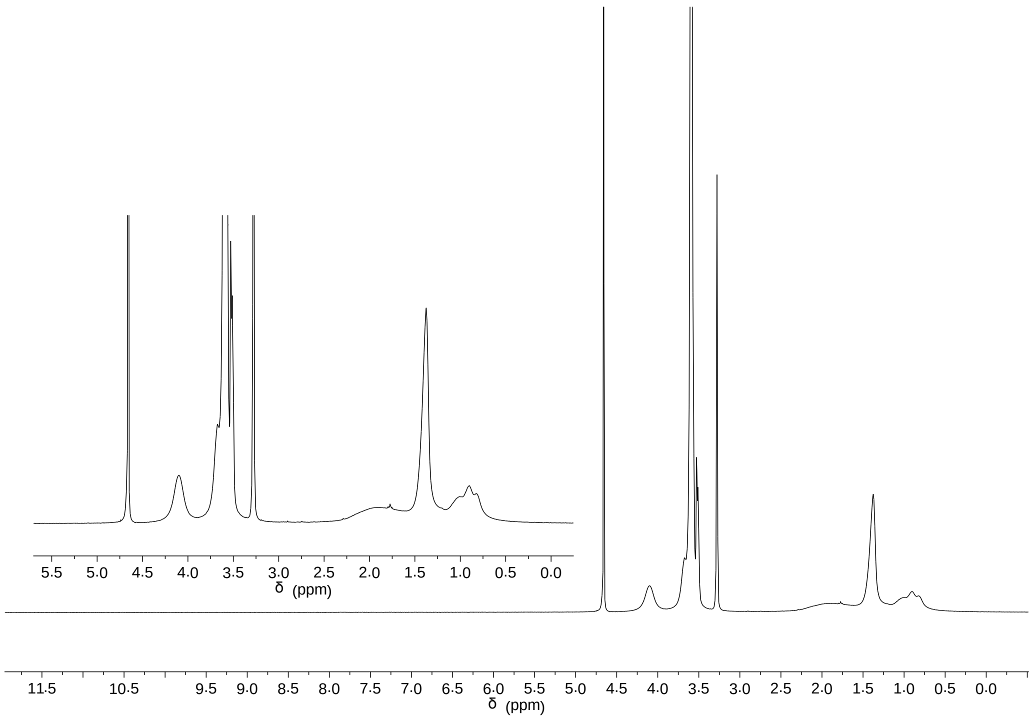

Fig. S31 [1]H NMR spectrum (300 MHz) of grafted PPEGMA$_{475}$-*co*-PAA in DMSO-d_6. The polymer was collected from Fe_3O_4@SiO_2@PPEGMA$_{475}$-*co*-PAA after treated with HF to remove the Fe_3O_4@SiO_2 core.

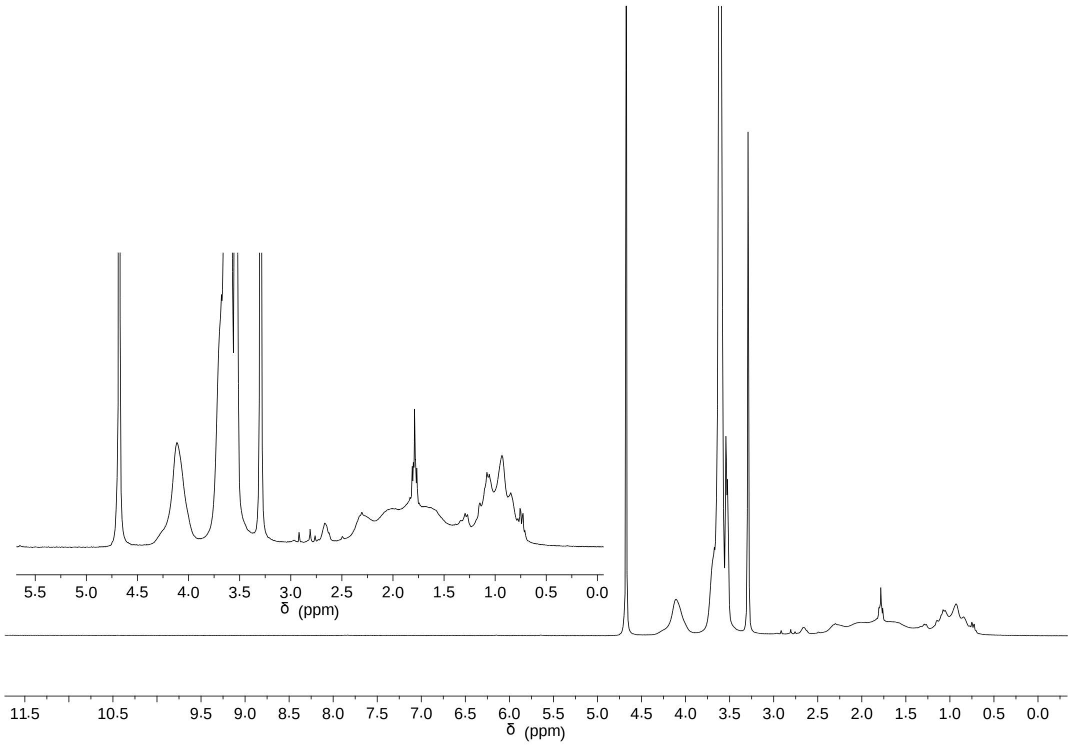

Fig. S32 [1]H NMR spectrum (300 MHz) of grafted PPEGMA$_{475}$-*co*-PAA in DMSO-d_6. The polymer was collected from Fe_3O_4@SiO_2@PPEGMA$_{475}$-*co*-PAA after treated with HF to remove the Fe_3O_4@SiO_2 core.

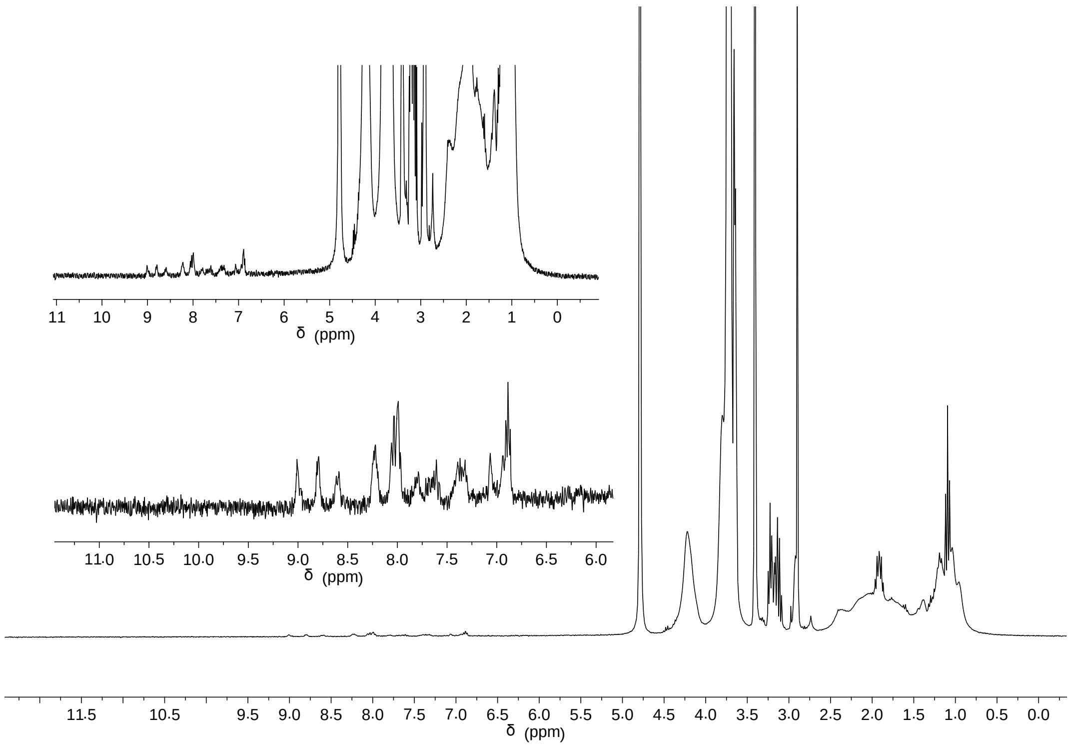

Fig. S33 ^{1}H NMR spectrum of grafted polymer in DMSO-d_6. The polymer was collected from Fe_3O_4@SiO_2@PPEGMA$_{475}$-*co*-PAA@Oxazine-2 after treated with HF to remove the Fe_3O_4@SiO_2 core.

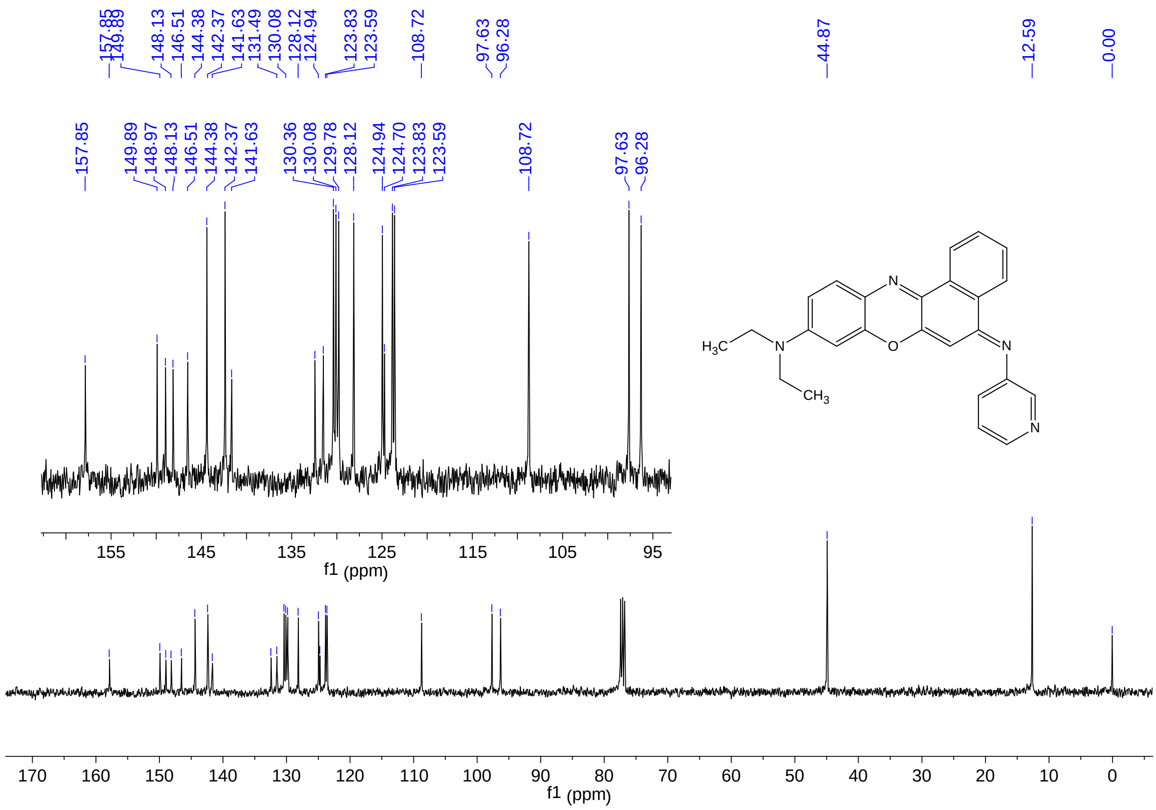

Fig. S34 ^{13}C NMR (75 MHz) of **2a** in $CDCl_3$.

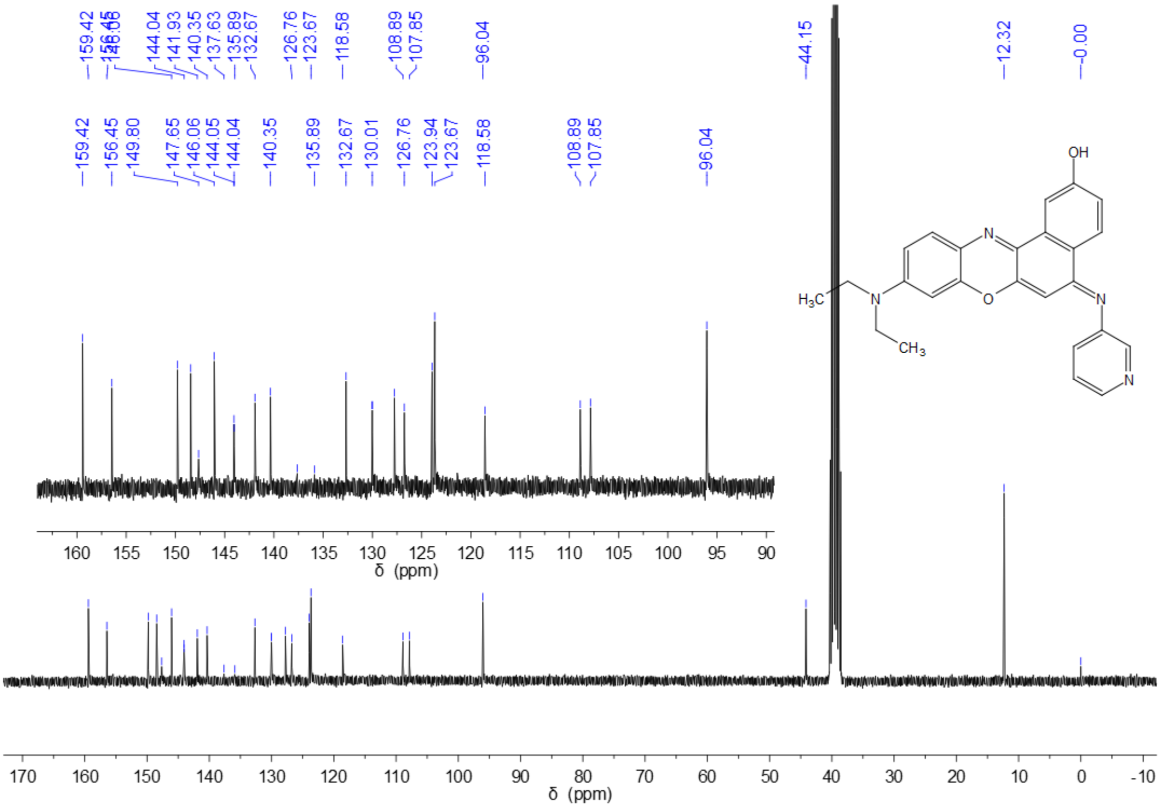

Fig. S35 ^{13}C NMR (75 MHz) of **2b** in DMSO-d_6.

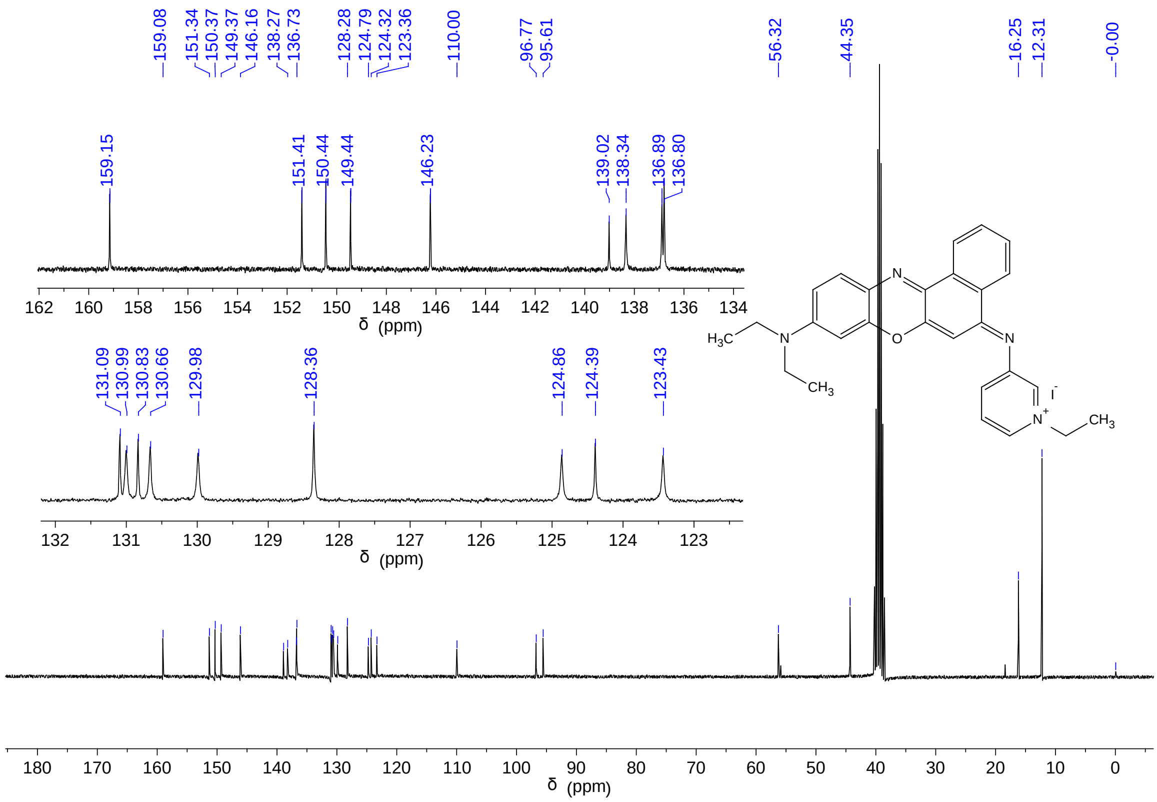

Fig. S36 ^{13}C NMR (75 MHz) of **3a** in DMSO-d_6.

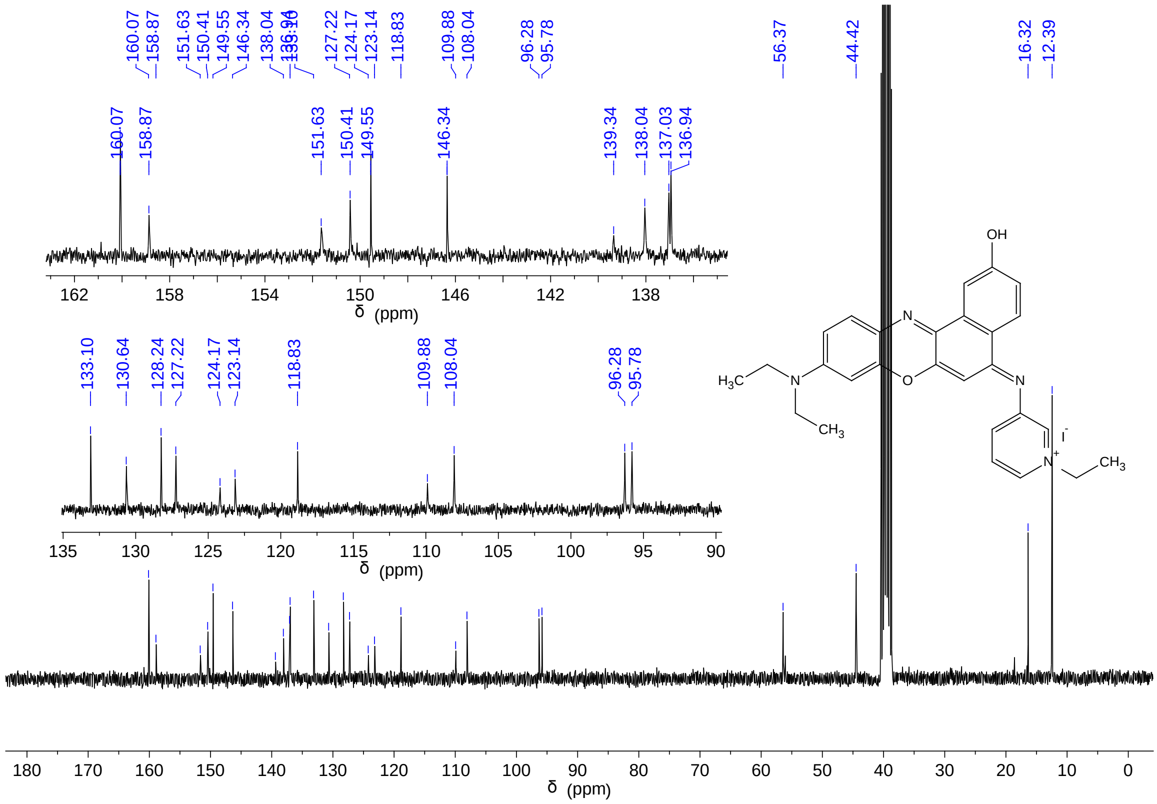

Fig. S37 ^{13}C NMR (75 MHz) of **3b** in DMSO-d_6.

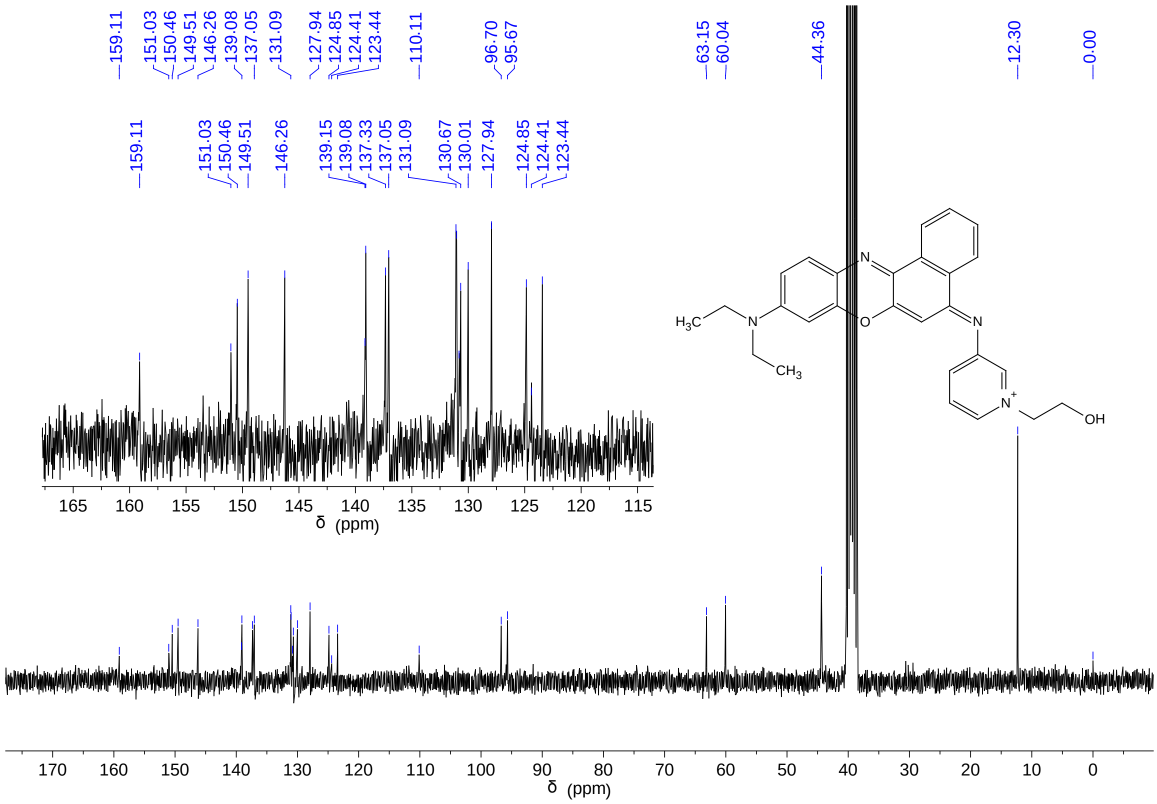

Fig. S38 ^{13}C NMR (75 MHz) of **3c** in DMSO-d_6.

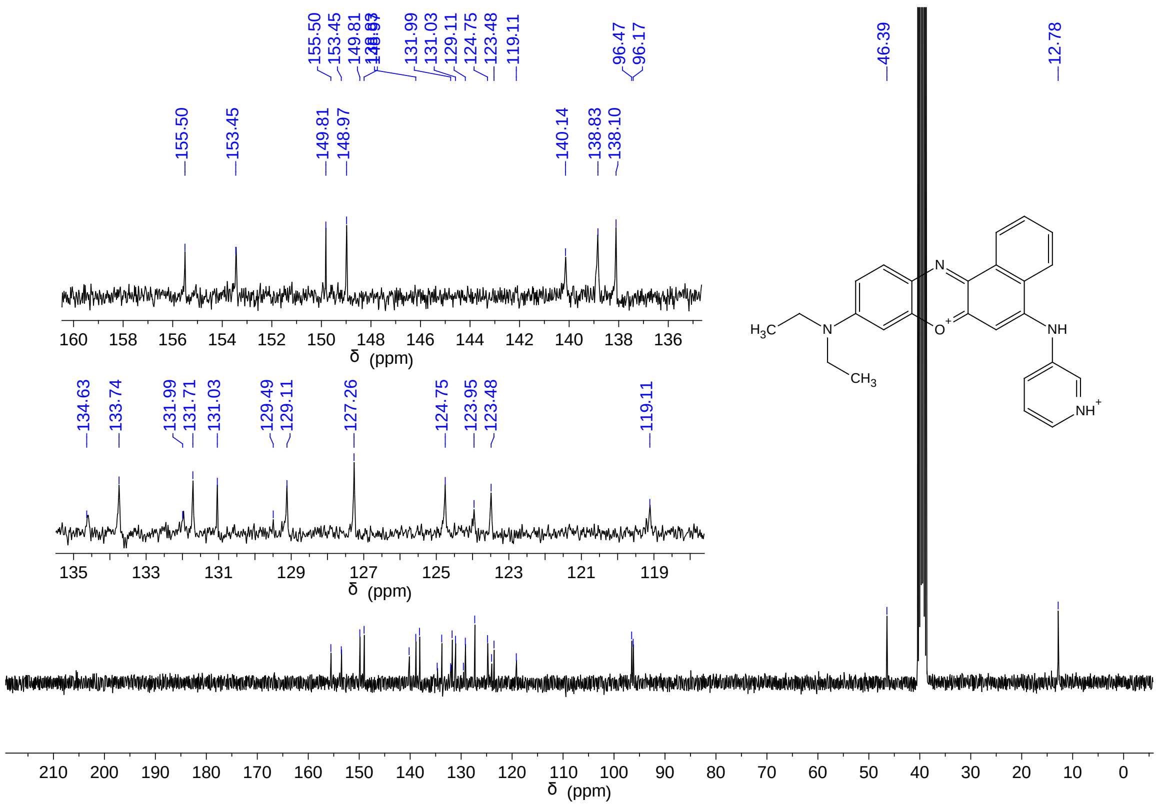

Fig. S39 ^{13}C NMR (75 MHz) of **2a+H$^+$** in DMSO-d_6.

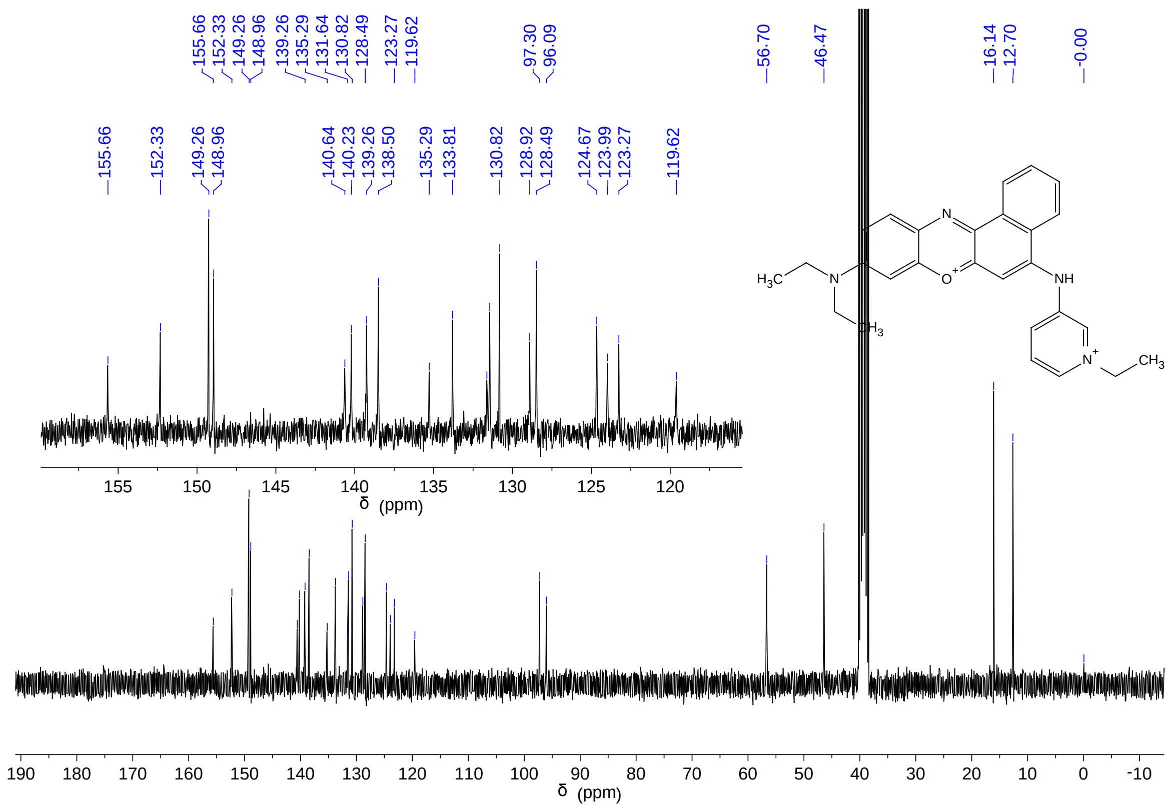

Fig. S40 ^{13}C NMR (75 MHz) of **3a+H$^+$** in DMSO-d_6.

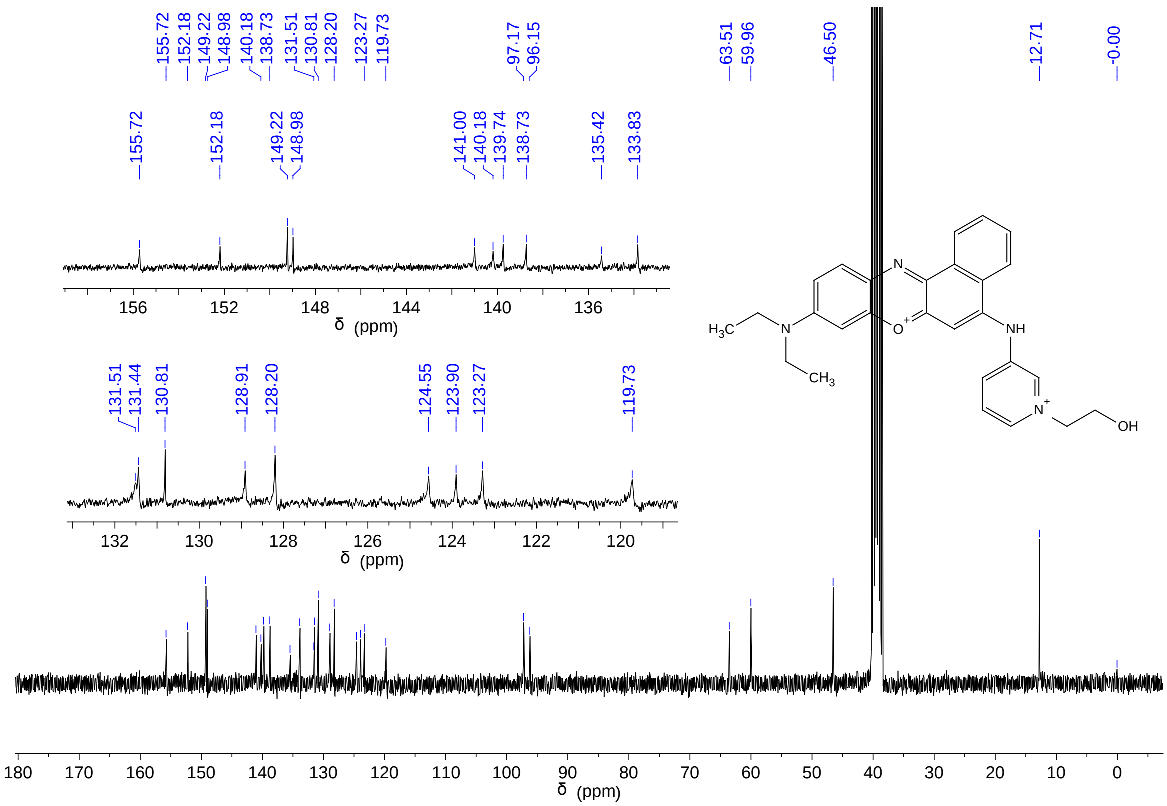

Fig. S41 ^{13}C NMR (75 MHz) of **3c+H$^+$** in DMSO-d_6.

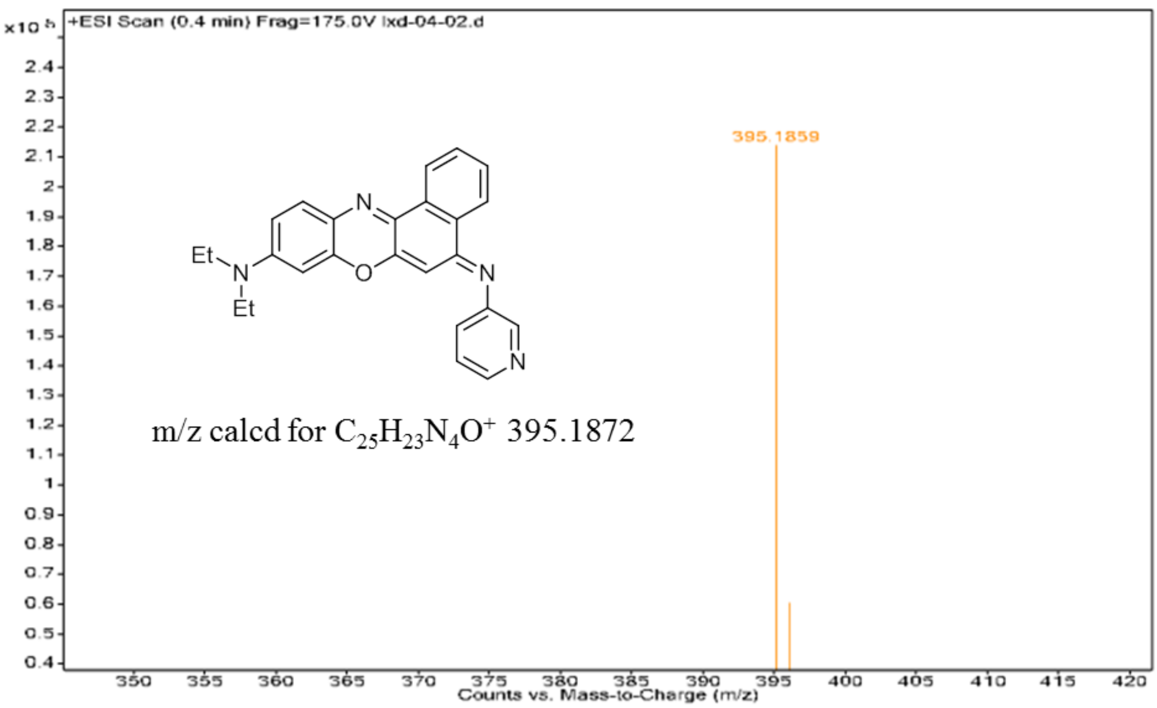

Fig. S42 HRMS of **2a**.

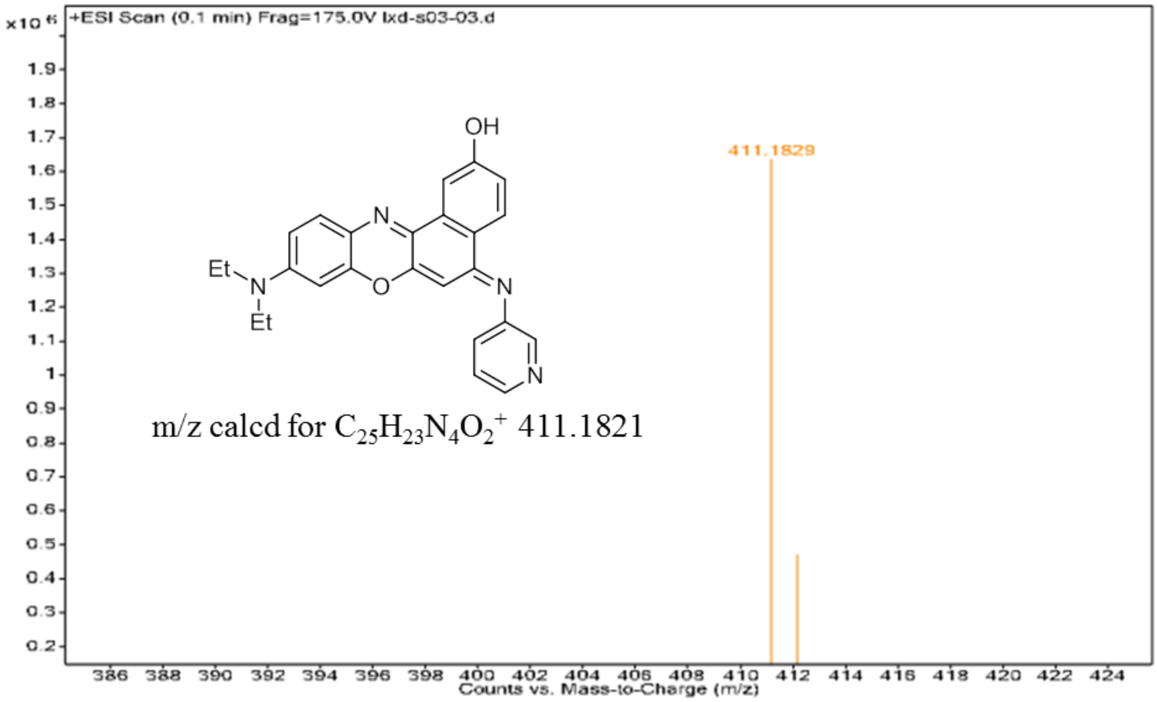

Fig. S43 HRMS of **2b**.

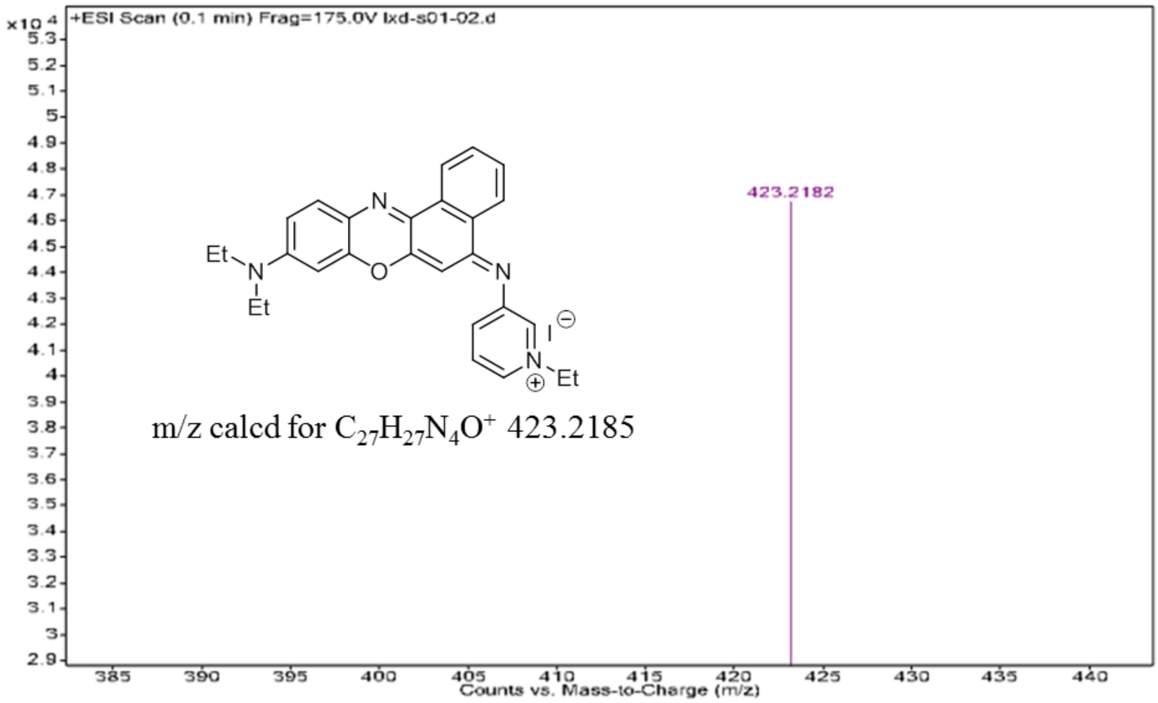

Fig. S44 HRMS of **3a**.

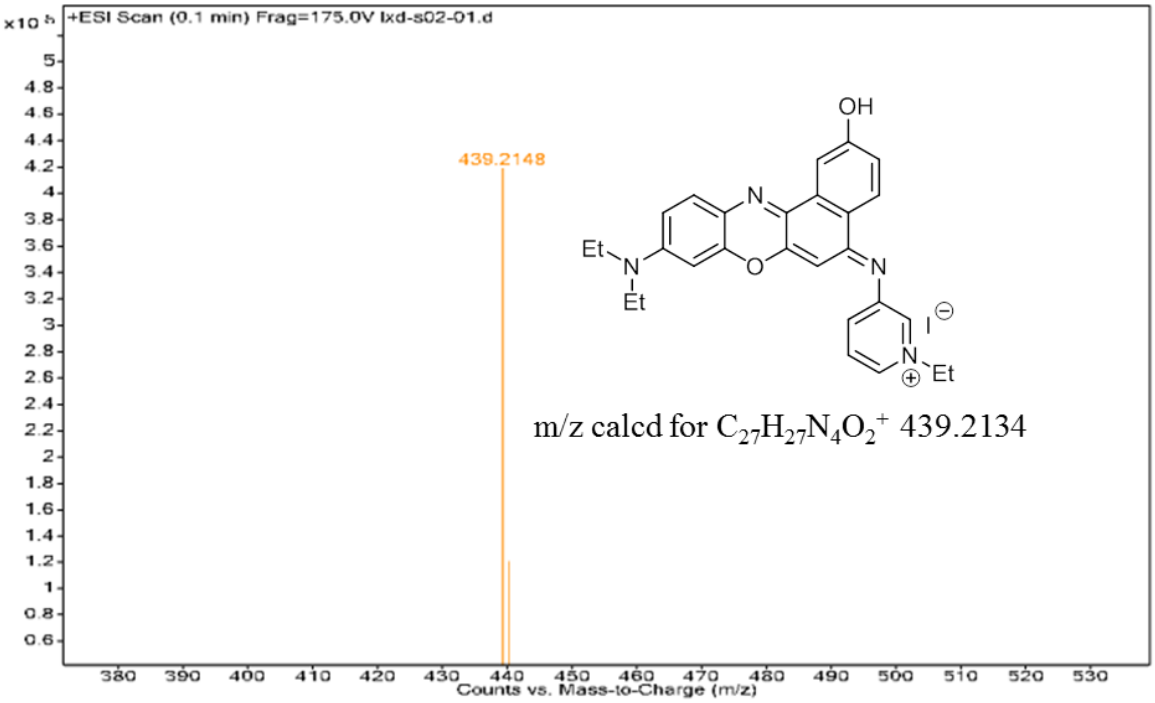

Fig. S45 HRMS of **3b**.

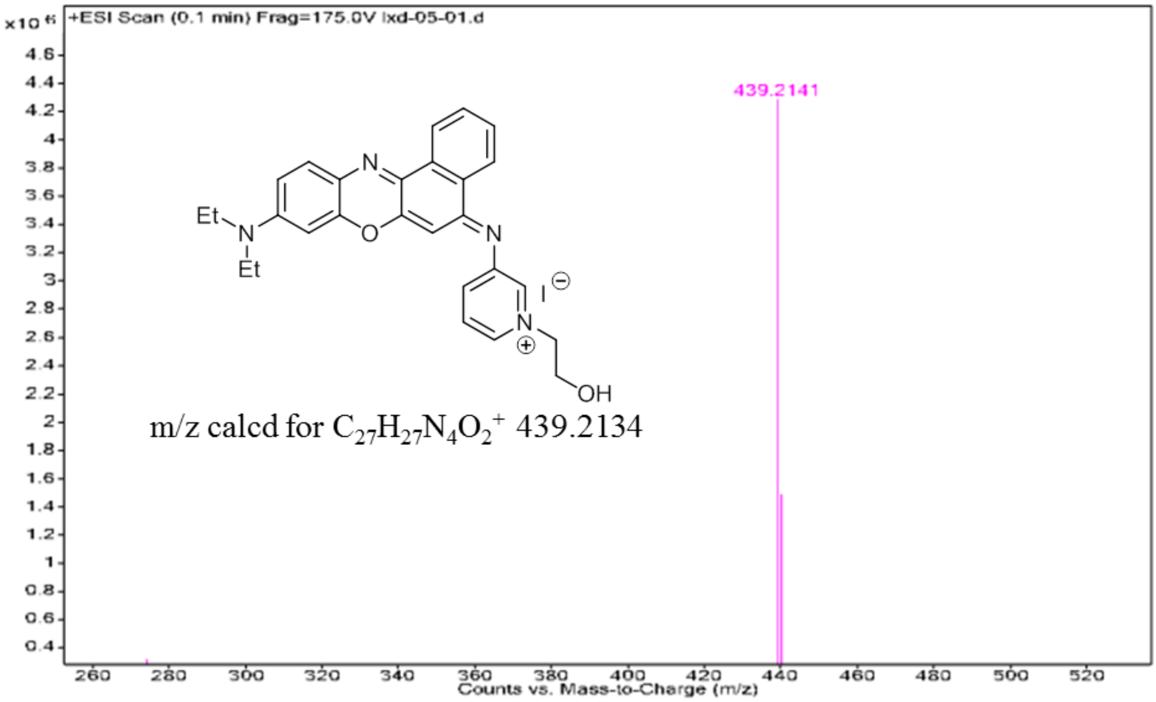

Fig. S46 HRMS of **3c**.

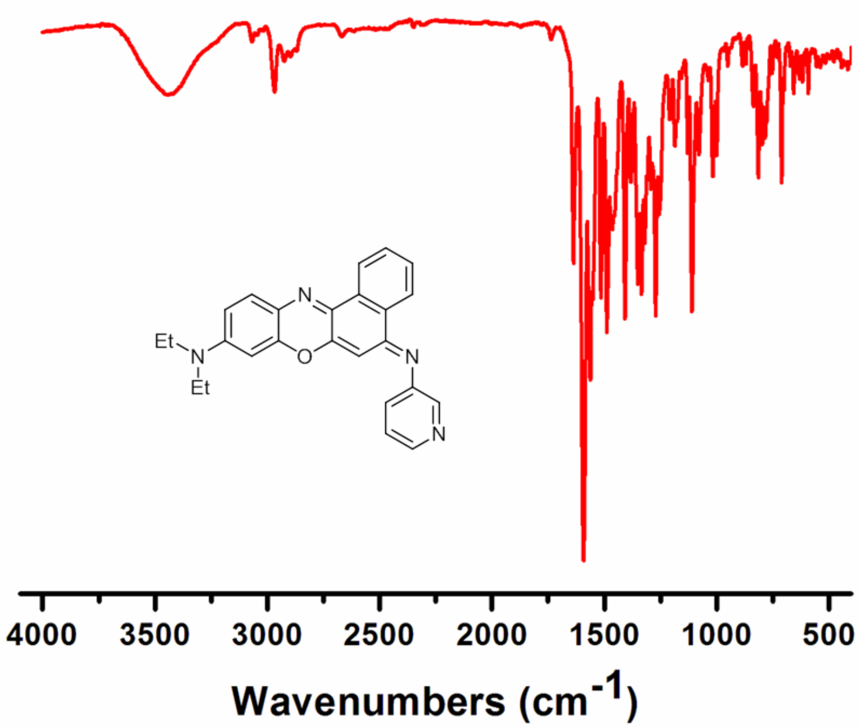

Fig. S47 FRTC of **2a**.

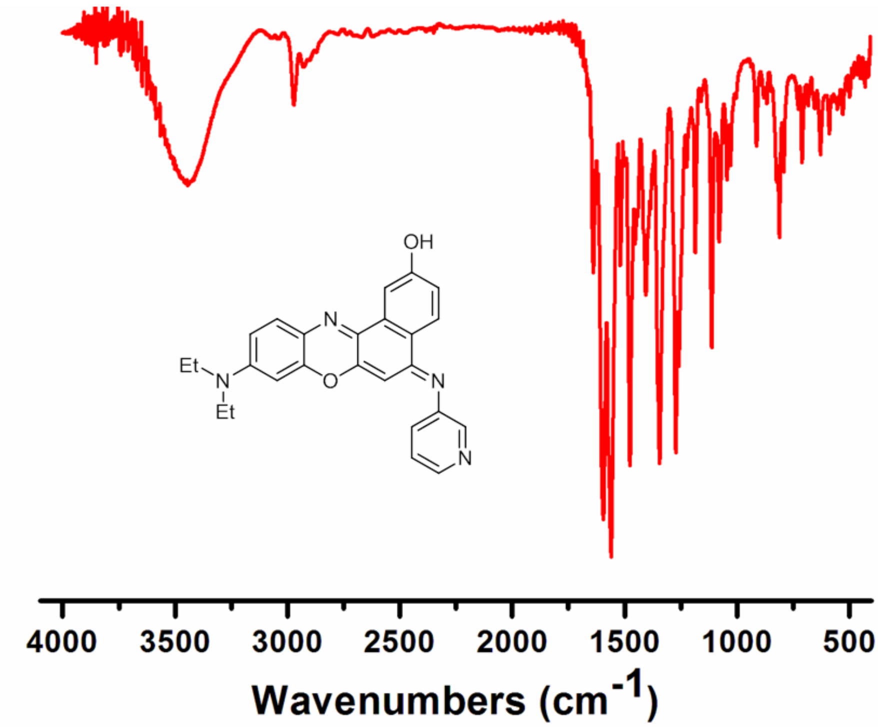

Fig. S48 FRTC of **2b**.

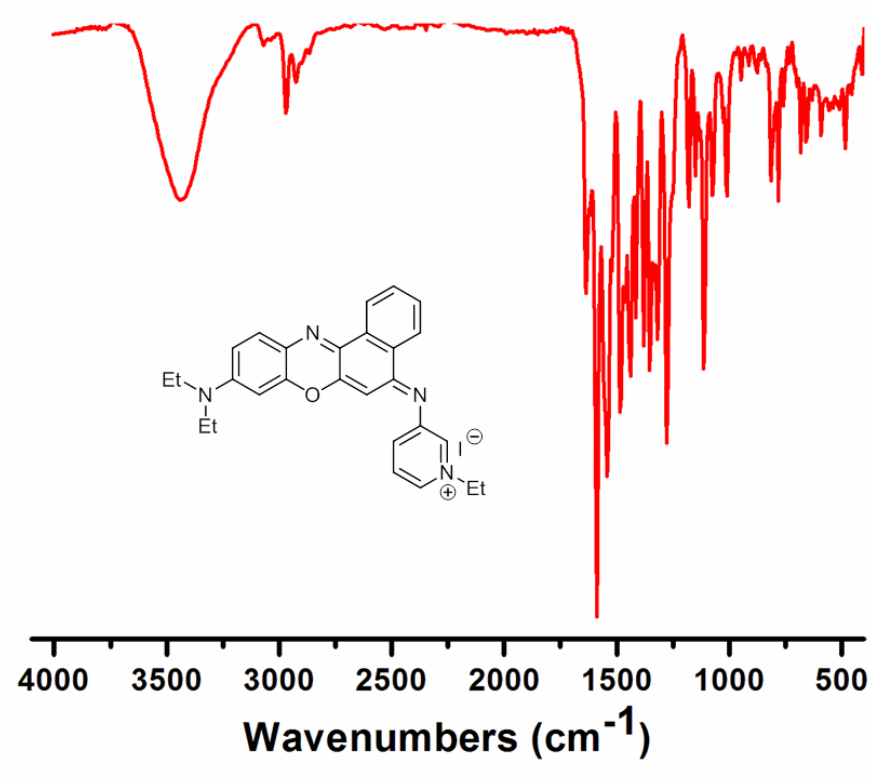

Fig. S49 FRTC of **3a**.

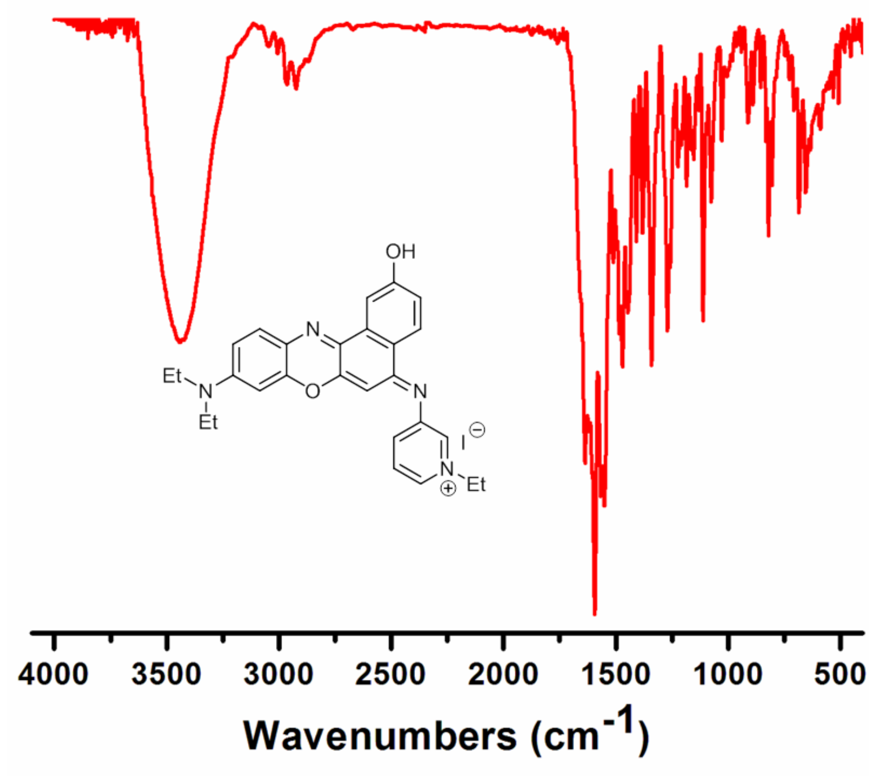

Fig. S50 FRTC of **3b**.

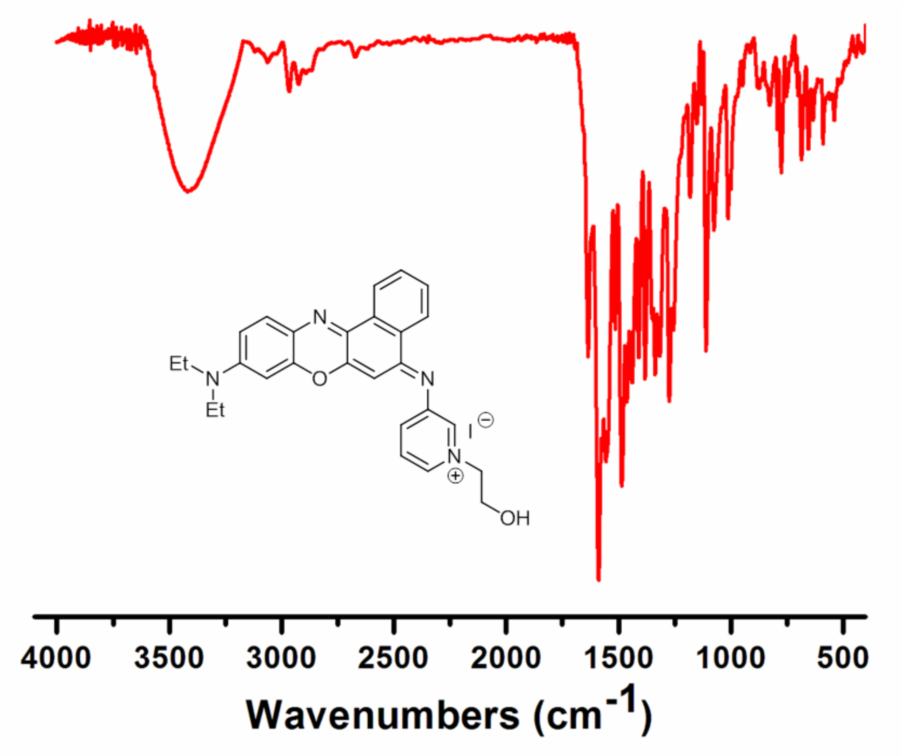

Fig. S51 FRTC of **3c**.